ISSN 2350-1030

International Journal of Recent Research in Physics and Chemical Sciences (IJRRPCS)
Vol. 10, Issue 2, pp: (13-40), Month: October 2023 – March 2024, Available at: www.paperpublications.org

Total Electron Content Variations at a Low Latitude East African Station and Its Comparison with IRI-2016, IRI-Plas2017 and NeQuick-2 Models during Solar Cycle 24.

Yusuf Olanrewaju Kayode[1,2*], Eugene Onori[2], Oluwafunmilayo Ometan[2], Sakiru Abiodun Okedeyi, Anthony Segara Ajose[1], Rafiu Bolaji Adegbola[2], Rasaq Adewemimo Adeniji-Adele[1]

[1]Department of Physics, Lagos State University of Education, Ijanikin, Lagos, Nigeria.

[2]Department of Physics, Lagos State University, Ojo, Lagos, Nigeria.

DOI: https://doi.org/10.5281/zenodo.10254820

Published Date: 04-December-2023

Abstract: **Ionospheric modelling is one of the most crucial approaches to study the activities of the ionosphere particularly in regions where experimental data are not readily available. This research aims to study the variations of Total Electron Content (TEC) in a low latitude east African station (Addis Ababa) by comparing experimental values of TEC from the Global Positioning System (GPS) with predicted data from IRI-2016, IRI-Plas2017 and NeQuick-2 models during solar cycle 24 using Root Mean Square Error (RMSE) and Mean Absolute Error (MAE) metric analysis approach. An hourly interval profile computed on seasonal basis were used to study the behaviors of TEC. A monthly interval error profile plotted on annual basis was also used to investigate the deviations of the models from the GPS values. This study analyzed TEC data from 2011 to 2017, utilizing 84 months of available data. The results from this study showed TEC have their lowest values during the post-midnight hours (02:00UT) and highest values during the pre-noon hours (11:00UT). We also observed that Equinoxes have high value of TEC than Solstices except during the ascending and maximum phases where seasonal/winter anomalies were recorded. From our statistical analysis, MAE was observed to give error value of ~3 TECU (TEC units) lower than the RMSE. Also from this result, we concluded that MAE is a better statistical metric than RMSE. IRI-Plas2017 outperformed IRI-2016 and NeQuick-2 models in predicting TEC values in East Africa during solar cycle 24, with a 71.4% better performance compared to other models.**

Keywords: **TEC. GPS. RMSE. MAE .IRI-2016 .IRI-Plas2017. NeQuick-2.**

1. INTRODUCTION

The ionosphere is a region of the Earth's upper atmosphere that contains a relatively high concentration of ions and free electrons [106], [65], [90], [92], [46]. It begins at an altitude of approximately 30 miles (50 kilometers) above the Earth's surface and extend to several hundred miles (several hundred kilometers). The ionosphere plays a crucial role in various atmospheric and electromagnetic phenomena and is of significant importance for radio wave propagation, telecommunications and space weather [87]. The ionosphere has different latitudinal regions which includes the high ,mid and low/equatorial regions. The equatorial/low latitude region is a distinct and most dynamic part of the Earth's ionosphere that spans the region around the Earth's equator [86], [30], [9], [108], [80], [39], [101], [51]. This region is characterized by unique ionospheric features and behavior due to its proximity to the equator and the interplay of various factors including solar radiation, geomagnetic effects, and atmospheric dynamics [77], [52], [59]. One of the prominent and unique features in this region is the Equatorial Ionization Anomaly (EIA). Equatorial Ionization Anomaly (E.I.A) refers to a specific pattern of electron density variations in the F2-layer of the ionosphere that is characterized by an increase in electron density during the daytime compared to the nighttime which is typically within about ±20° latitude from the equator [35], [70], [110], [7], [1], [84], [2], [69], [120], [3]. A physical mechanism known as the E X B drift is related to the mobility of charged particles (ions and electrons) in the ionosphere of the Earth as a result of the combined electric (E) and magnetic (B) fields present in that area of the atmosphere [43]. The E X B drift is an essential phenomenon to comprehending the motion and distribution of charged particles in the low latitude/equatorial region of the ionosphere, including their motion and distribution [3]. The effects of this motion on phenomena including the development of ionospheric plasma structures, the motion of plasma bubbles, and the influence on radio wave propagation and communication systems can all be considered [19]. To comprehend ionospheric dynamics and its effects on numerous technologies that depend on ionospheric conditions, researchers and scientists examine the E x B drift [39]. This unique feature and many other ionospheric dynamics leads large fluctuations in the radio wave along the satellite propagation signal paths [113], [62], [19], [6]. These fluctuations in signals will in turns lead to ionospheric delay error in signals which will invariably cause variations in ionospheric parameters such as electron or Total Electron Content (TEC). Total Electron Content (TEC) is the number of electrons present along the path between the satellite transmitter and ground base receiver [9], [13], [112], [111], [91]. This delay experienced by the signals travelling through the ionosphere along the signal path between the satellite and the receiver on the ground is proportional to TEC [114], [37], [54], [41], [18]. Therefore, the differential GPS signal delay (psedo-range) or the differential phase advance (carrier phase measurements) of the dual frequencies (1.5754 GHz and 1.2276 GHz) can be applied to derive the TEC along the signal path [4], [113], [86]. Apart from the GPS measurements of TEC, empirical models such as IRI, IRI-Plas and NeQuick models are widely used to study the variations of the ionospheric parameters (such as TEC) particularly in areas real-time measurements are not available [87], [104], [21], [48], [50], [94], [56]. There have been several ionospheric models used in predicting the true state of the ionosphere but their optimal performances are still a major setback in low/equatorial region particularly in the African region. This problem is due to the scarcity of real time input data in the models [79], [64]. Ionospheric modelling is important because it is a major tool in space weather prediction, navigations and surveillance systems [38], [28], [55], [75].

One of the most common and widely used model is the International Reference Ionosphere (IRI), meanwhile this model is updated from time to time. The International Reference Ionosphere (IRI) model is a global model developed by the International Union of Radio Science (URSI) and Committee on Space Research (COSPAR) [23], [24], [25]. The IRI model provides a reference representation of the ionosphere based on a combination of measured data and empirical formulae. It covers a wide range of ionospheric parameters such as electron density, electron temperature, and ion composition. [16], [22].

The NeQuick is an ionospheric model that is specifically designed for the predictions of electron density in the ionosphere. It was developed by the European Space Agency (ESA) and the European Telecommunication Standard Institutes (ETSI) for radio wave propagation and communication system design purposes [100], [117], [82].

[32] established that both IRI and NeQuick-2 models has same level of performance in the oceania region. They also compared their results with experimental results from Jason2/3 ionospheric data between 2002 to 2018. They concluded that IRI and NeQuick-2 models underestimate TEC but reflect long-term average condition of the ionosphere. [116] reported in their work that IRI-2016 is a good climate model that can provide accurate estimates of ionospheric delays of radio signal propagated over Pakistan in the Asian sector during the descending phase of solar cycle 24 (2015-2017). They also affirmed in their study that IRI-2016 model shows a better agreement with measured TEC around 06:00UT- 12:00UT. [105] also carried out a research at Pakistan and they came to conclusion that IRI-2016 model performed better IRI-2007 and IRI-2012 models in monthly values of TEC during the descending phase of solar cycle 24 (2019-2020). [16] reported that IRI-2016 and IRI-Plas2017 models are not superior to each other in comparison with experimental TEC (Ionolab) when the plasmapheric effect are neglected and their predictive power depends on availability of data. Meawhile, [16] still further stated that IRI-2001 topside option of the IRI-2016 model is better in predicting TEC than the IRI01-Corr and NeQuick topside option at Instanbul (Turkey). [45] also reported in their work that IRI-Plas2017 performs better than NeQuick-2

model for low latitude stations during June solstice while the reverse was observed for high latitude station, meanwhile during September equinox their performance does not follow a definite pattern as observed in other seasons. In the work of Bolaji et al. (2017), they concluded that the NeQuick-2 model does not have the capability to predict the EIA crest pattern in northern or southern hemisphere in the African region. [87] uses GNSS/GPS data to assess the performance of IRI-Plas2017 and NeQuick-2 models in six different longitudinal sectors covering 36 GNSS receiver stations for a period of 2006 to 2017 (4497 months of available data) and they concluded from their results that NeQuick-2 model performed better in 83% of the months while IRI-Plas2017 had 17% performance. [86] adopted the comparative analysis of IRI-2016 and IRI-Plas2017 models with GPS-TEC in the Europe, Africa and Asia longitude and they concluded that IRI-2016 performs better than IRI-Plas2017 in all the longitudinal sectors. [85] in their own research reported that Observed-TEC (OBS-TEC) and IRI-2016 model VTEC rise from a minimum value in the early hours to broad day time maximum before falling steeply to another minimum after sunset in African (Nigeria). They attributed this phenomenon to photoionization increase produced by solar Extreme Utraviolet (EUV) radiation. They also concluded that IRI-2016 model cannot be used as a proxy for TEC measurements for most hours of the day in Birni Kebbi (Nigeria).

Many other researchers like [20], [5], [4], [11], [14], [16], [8], [31], [83], [115], [12], [113], [76], [71], [86], [107], [53], [78], [95], [119] have studied the variations of TEC with comparison with IRI and NeQuick models in different longitudinal sectors. In recent time, only few researches have been presented in the low/equatorial latitude east African region due to its dynamic, complex nature and unavailability of measurement data hence, the need for more investigations. This paper will study the variations of TEC in a low latitude east African GPS station by comparing experimental values of TEC (GPS-TEC) with predicted TEC from IRI-2016, IRI-Plas2017 and NeQuick-2 models during three different phases (ascending, maximum, and descending) of solar cycle 24 using two different standard metric of measurement (RMSE and MAE). The results from this research will reveal the predictive level of IRI and NeQuick models and suggest their possible upgrade and update which will make the study of ionospheric activities easier even in areas where GPS stations are not present in the African sector.

2. DATA AND METHOD OF ANALYSIS

In this research work, the two types of ionospheric data used were the observed data, which is the GPS-TEC, and the predicted ionospheric data from an East Africa GPS station, Addis Ababa (ADIS) between 2011 to 2017, with coordinates of geographic longitude and latitude of 38.77°E, 9.04°N, and geomagnetic longitude and latitude of 110.83°E, 31.75°N, respectively. The observed data is the GPS data, which is obtained from the University NAVSTAR Consortium (UNAVCO) website at http://www.unavco.org, while the predicted data used in this research work are the IRI-2016, IRI-Plas2017, and the NeQuick-2 models. The NeQuick-2 model is an improved and updated version of the NeQuick model [82], [99], [96].The hourly TEC values of IRI-2016 were obtained from the Community Coordinating Modeling Center (CCMC) website (https://ccmc.gsfc.nasa.gov/modelweb/models/iri2016_vitmo.php) using IRI-2001 topside option. The IRI-Plas 2017 computes TEC data up to a height of 20,200km. Also, hourly TEC values for the IRI-Plas 2017 model were obtained using the windows executable program from the website of the IZMIRAN Institute (http://ftp.izmiran.ru/pub/izmiran/SPIM/) [16]. While, hourly TEC values of NeQuick-2 were obtained using the windows executable program created from the FORTRAN source code, which was obtained from the Ionosphere Radio Propagation Unit of the T/ICT4D Laboratory (https://t-ict4d.ictp.it/nequick2/source code). GPS-TEC were downloaded in Receiver Independent Exchange (RINEX) format and were processed using GPS-TEC analysis software (GPS_Gopi_v3.03), designed and developed by Gopi Seemala of the Indian Institute of Geomagnetism and accessible from his webpage (https://seemala.blogspot.com). The summary of the GPS-TEC application software is to read raw data from the RINEX file, process cycle slips, multipath, and scintillations, and then produce output TEC values [87], [85]. According to [86] and [101], an elevation cut-off angles greater than 50° is required for an ionospheric shell height of about 350km for the low/equatorial-latitude region of the ionosphere. GPS-TEC obtained from the GPS-TEC analysis software are in per minute sequence, which were averaged to hourly TEC values using equation 1. Also, equation 1 was used to convert hourly TEC values of IRI-2016, IRI-Plas 2017 and NeQuick-2 models to monthly TEC values.

$$\bar{x} = \frac{1}{n}\sum_{i=1}^{n}(TEC_i) \qquad (1)$$

The hourly values of GPS-TEC, IRI-2016, IRI-Plas 2017 and NeQuick-2 were used to study the diurnal variations in TEC. Furthermore, the hourly TEC values were averaged to daily values and further averaged to monthly values. The monthly

ISSN 2350-1030

International Journal of Recent Research in Physics and Chemical Sciences (IJRRPCS)
Vol. 10, Issue 2, pp: (13-40), Month: October 2023 – March 2024, Available at: www.paperpublications.org

TEC values were further grouped into the four seasons namely: March equinox (February, March, and April), June solstice (May, June, and July), September equinox (August, September, and October) and December solstice (November, December, and January) as shown in Table 1, in order to analyze the seasonal variations in TEC.

Table 1: The four Seasons of the year with their corresponding months.

S/N	Seasons	Months
1	*March Equinox*	*February, March, April*
2	*June Solstice*	*May, June, July*
3	*September Equinox*	*August, September, October*
4	*December Solstice*	*November, December, January*

To investigate the performances of the ionospheric models, the Root Mean Square Error (RMSE) and Mean Absolute Error (MAE) were used.

RMSE is calculated using equation 2.

$$RMSE = \sqrt{\sum_{i}^{N} \frac{(TECmodel_i - TECgps_i)^2}{N}} \quad (2)$$

Where $TECmodel_i$ is the TEC data from IRI-2016, IRI-Plas2017 and NeQuick-2 models while $TECgps_i$ is the TEC data from GPS and N is the number of hours per day.

The MAE was calculated using equation 3.

$$MAE = \left[n^{-1} \sum_{i}^{n} (y_i - x_i)\right] \quad (3)$$

where y_i is the prediction, x_i true value and n is the total number of data points.

The Percentage Deviation is the degree of how the models deviated from the GPS-TEC value given by equation 4

$$percentage\ Deviation = \left(\frac{GPS - Model}{GPS}\right) X100 \quad (4)$$

TEC Deviation is also employ to investigate the difference in the TEC value between the GPS and modelled TEC and given by equation 5

$$\text{TEC Deviation} = GPS_{observed} - Model_{predicted} \quad (5)$$

Table 2: The years, Solar Cycle Phase and Sunspot number.

S/N	Years	Solar Cycle Phase	Sunspot Number(R_z)
1	2011	*Ascending*	55.6
2	2012	*Ascending*	57.6
3	2013	*Ascending*	64.7
4	2014	*Maximum*	79.6
5	2015	*Maximum*	69.9
6	2016	*Descending*	39.9
7	2017	*Descending*	21.8

3. RESULTS AND DISCUSSIONS

3.1 Diurnal and Seasonal Variations in TEC

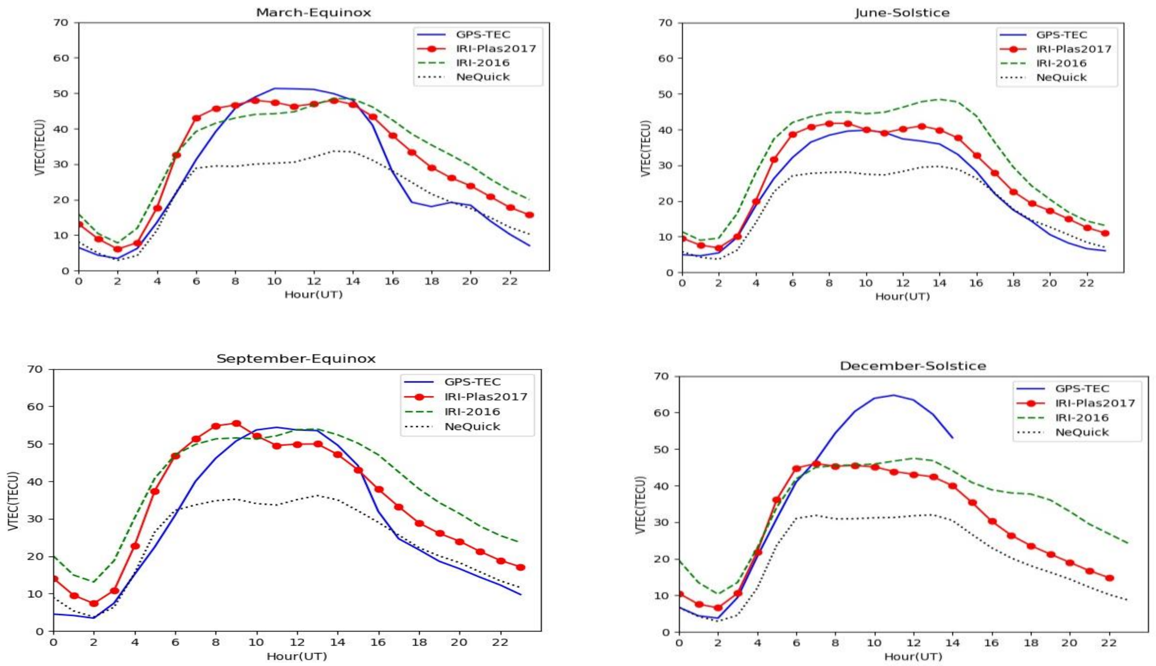

Fig. 1 Diurnal and Seasonal Variations in TEC at ADIS in 2011

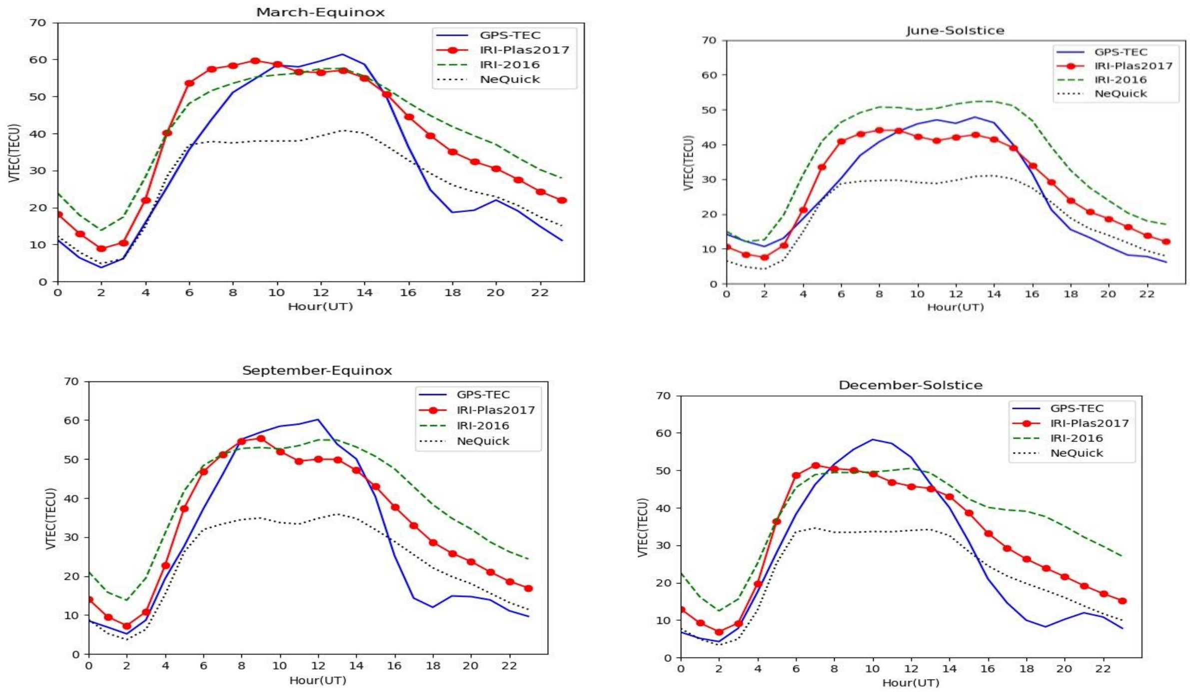

Fig. 2 Diurnal and Seasonal Variations in TEC at ADIS in 2012

International Journal of Recent Research in Physics and Chemical Sciences (IJRRPCS)
Vol. 10, Issue 2, pp: (13-40), Month: October 2023 – March 2024, Available at: www.paperpublications.org

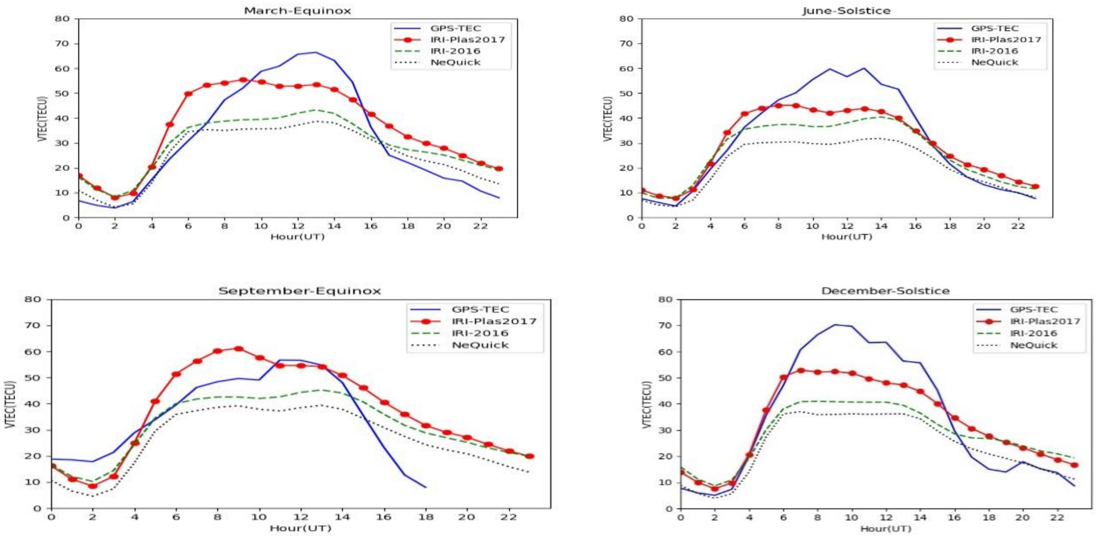

Fig. 3 Diurnal and Seasonal Variations in TEC at ADIS in 2013

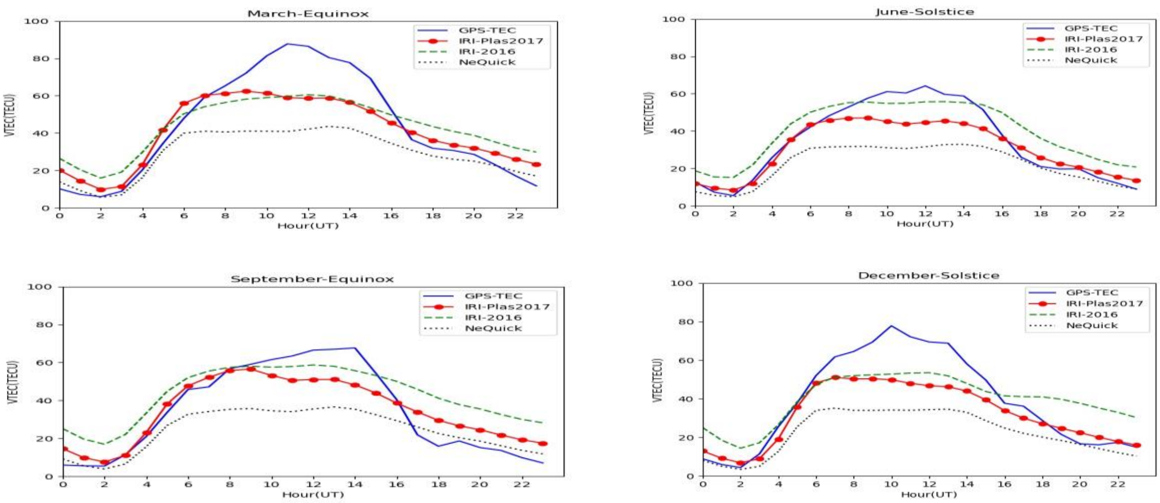

Fig. 4 Diurnal and Seasonal Variations in TEC at ADIS in 2014

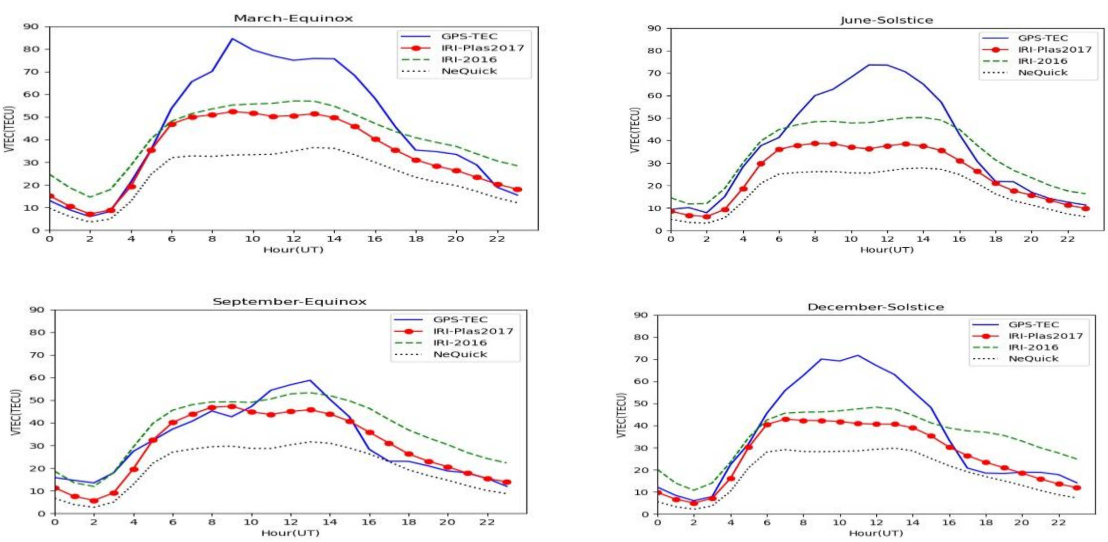

Fig. 5 Diurnal and Seasonal Variations in TEC at ADIS in 2015

ISSN 2350-1030

International Journal of Recent Research in Physics and Chemical Sciences (IJRRPCS)
Vol. 10, Issue 2, pp: (13-40), Month: October 2023 – March 2024, Available at: www.paperpublications.org

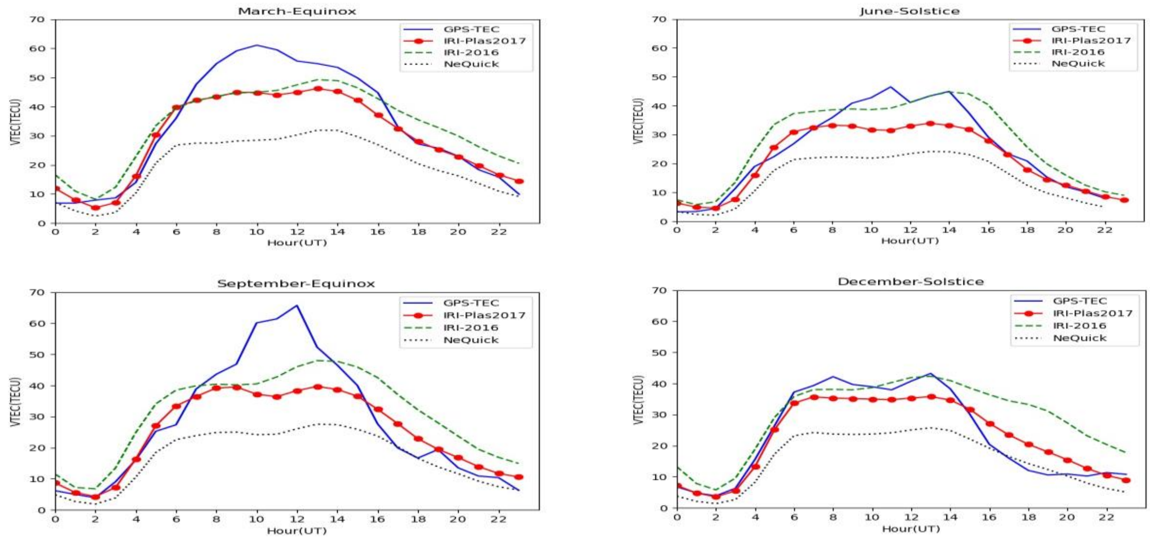

Fig. 6 Diurnal and Seasonal Variations in TEC at ADIS in 2016

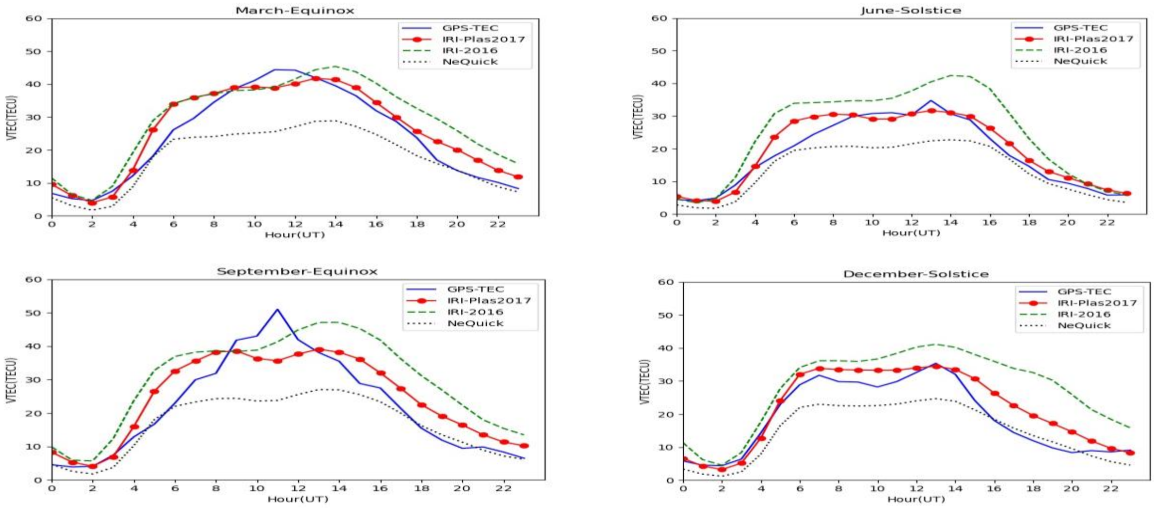

Fig. 7 Diurnal and Seasonal Variations in TEC at ADIS in 2017

Fig. 1-7 shows the diurnal and seasonal variations in TEC between 2011 to 2017. The years 2011 to 2013 is the ascending solar activity phase. In this solar cycle phase, GPS-TEC experiences equinoctial asymmetry, except in 2012 where it was pronounced during the March equinox for GPS-TEC values. Equinoctial asymmetry is a phenomenon whereby the two equinoxes (March and September Equinox) records different range values of TEC [40], [44], [102], [27], [72]. This is as a result of the differences in the meridional winds which in turn leads to changes in the neutral gas composition during equinoxes [85], [73]. Equinoctial asymmetry can also be attributed to the fact that the height of F layer is higher during vernal equinox as compared to autumn equinoxes [109], [43]. The IRI-2016 and IRI-Plas2017 models mostly overestimate GPS-TEC during the morning hours (02:00UT-06:00UT) and night period (15:00UT-23:00UT) of the day. The NeQuick-2 had a good agreement with GPS-TEC during the early morning hours of the day (01:00UT-06:00UT). The IRI-2016, IRI-Plas2017 and NeQuick-2 models mostly underestimates GPS-TEC around the noon period (12:00UT). The highest overestimations of GPS-TEC recorded during this solar cycle phase was also around the noon period particularly during the June solstice. The IRI-Plas2017 model slightly overestimates GPS-TEC around the noon period during the equinox months except during the September equinox month in 2013 where it recorded ~5 TECU higher than the GPS-TEC. The years 2014 and 2015 recorded the highest average annual sunspot number which makes the values of TEC to be higher than other solar cycle phases. The highest peak value of GPS-TEC was recorded during the March equinox season of both years as ~85 TECU while the highest values of IRI-2016, IRI-Plas2017 and NeQuick-2 models were recorded as ~60 TECU, ~61 TECU

International Journal of Recent Research in Physics and Chemical Sciences (IJRRPCS)
Vol. 10, Issue 2, pp: (13-40), Month: October 2023 – March 2024, Available at: www.paperpublications.org

and 41 TECU respectively. Semi Annual variation anomaly was recorded during this maximum phase (2014 and 2015) due to the slightly lower values of TEC recorded during the September equinox when compared to the equinox seasons. This phenomenon is attributed to the fact the solar zenith angle of sun is lower during the equinox season and higher during the solstice seasons [60], [98]. The descending phase of the solar cycle (2016 and 2017) experiences a fall in the value of TEC which was as a result of drop in the sunspot number [49], [89], [15], [93], [66], [97]. The highest peak value of TEC recorded in this phase was ~67 TECU during the September equinox around the noon period (12:00UT) from the GPS-TEC while the lowest value of TEC recorded was observed from the NeQuick-2 model around the post-midnight period (02:00UT). This lowest value was recorded as ~3 TECU around the same time frame for all seasons and in all the solar cycle phases from the NeQuick-2 model in this research. Generally, winter anomaly was observed in all the phases of the solar cycle except during the descending phase. Winter anomaly is a phenomenon where the December solstice TEC value is greater than the June solstice [57], [42], [90], [67]. This is as a result of the variations in the neutral composition (O/N_2 ratio) at thermospheric height [85],[36], [88], [118]. Night time enhancement was also observed in all the phases of the solar cycle which is as a result of irregularities in the electron distributions in the F-region of the ionosphere during the night period [74], [17], [68], [33]. This physical phenomenon is more pronounced and stronger during the ascending phase and weakest during the descending phase. Equatorial noon bite-out is another prominent phenomenon observed mostly during the June and December solstice during the ascending and maximum/descending phases of the solar cycle. It is a physical mechanism that is most observed in the equatorial low latitude region in the ionosphere, which is as a result of EXB drift leading to fountain effect in the F-region [61], [34], [58], [81]. Generally, the IRI and NeQuick models manifested a daytime underestimations and nighttime overestimations of TEC, which is similar to the results reported by [103] and [114].

3.2 Percentage Deviations of IRI-2016, IRI-Plas2017 and NeQuick-2 models from GPS-TEC

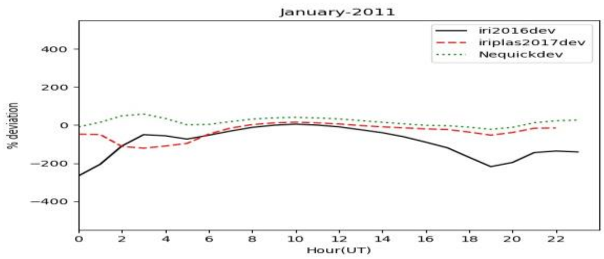

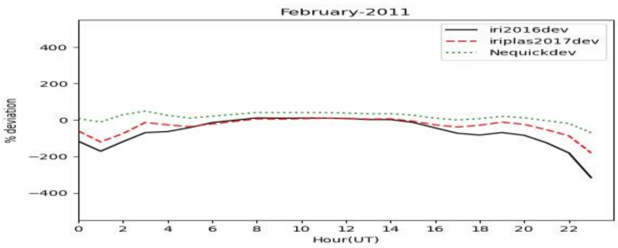

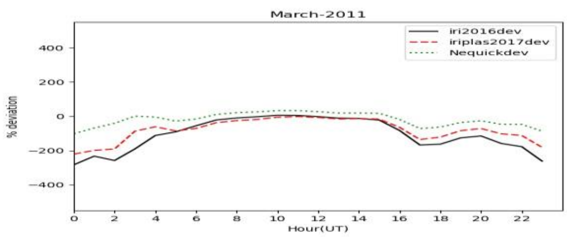

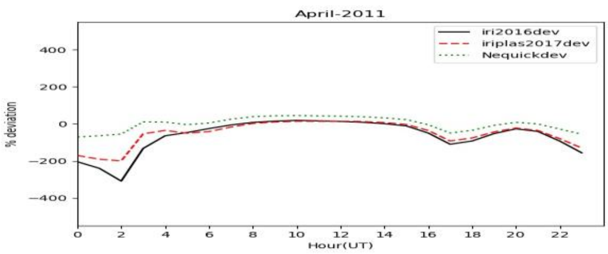

International Journal of Recent Research in Physics and Chemical Sciences (IJRRPCS)
Vol. 10, Issue 2, pp: (13-40), Month: October 2023 – March 2024, Available at: www.paperpublications.org

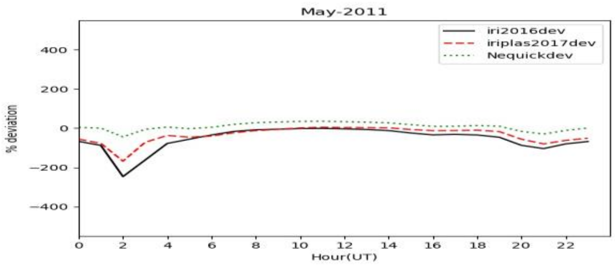

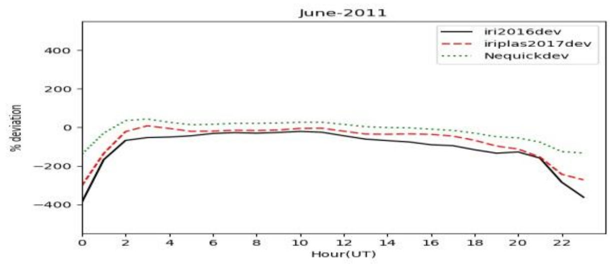

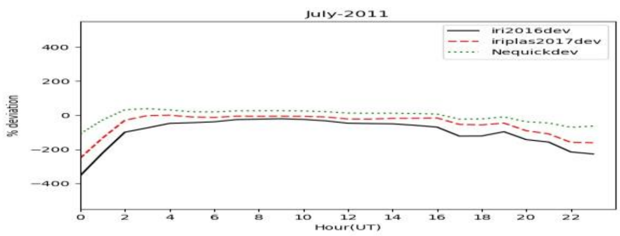

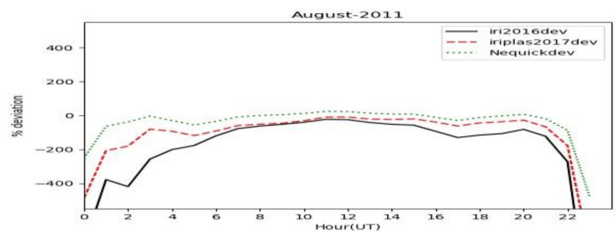

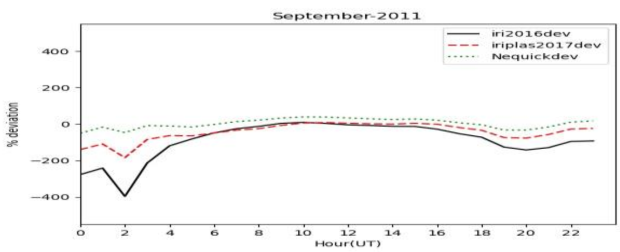

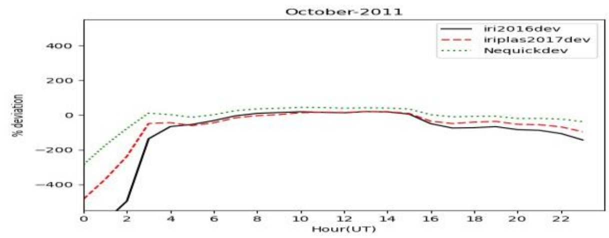

ISSN 2350-1030

International Journal of Recent Research in Physics and Chemical Sciences (IJRRPCS)
Vol. 10, Issue 2, pp: (13-40), Month: October 2023 – March 2024, Available at: www.paperpublications.org

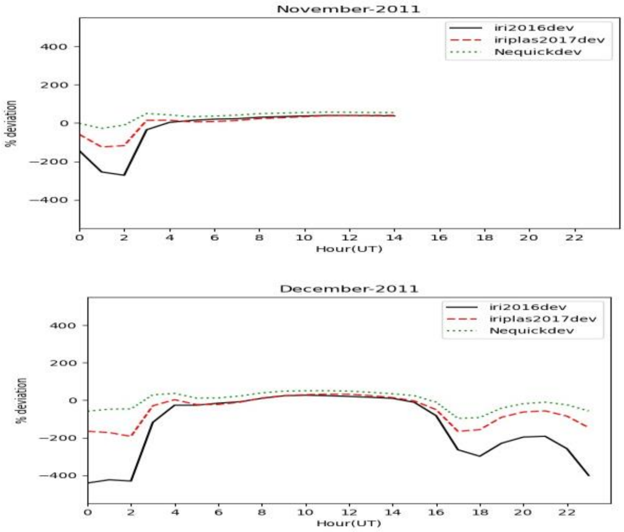

Fig. 8 Monthly Percentage Deviations of IRI-2016, IRI-Plas2017, and NeQuick-2 models from GPS-TEC during the ascending phase

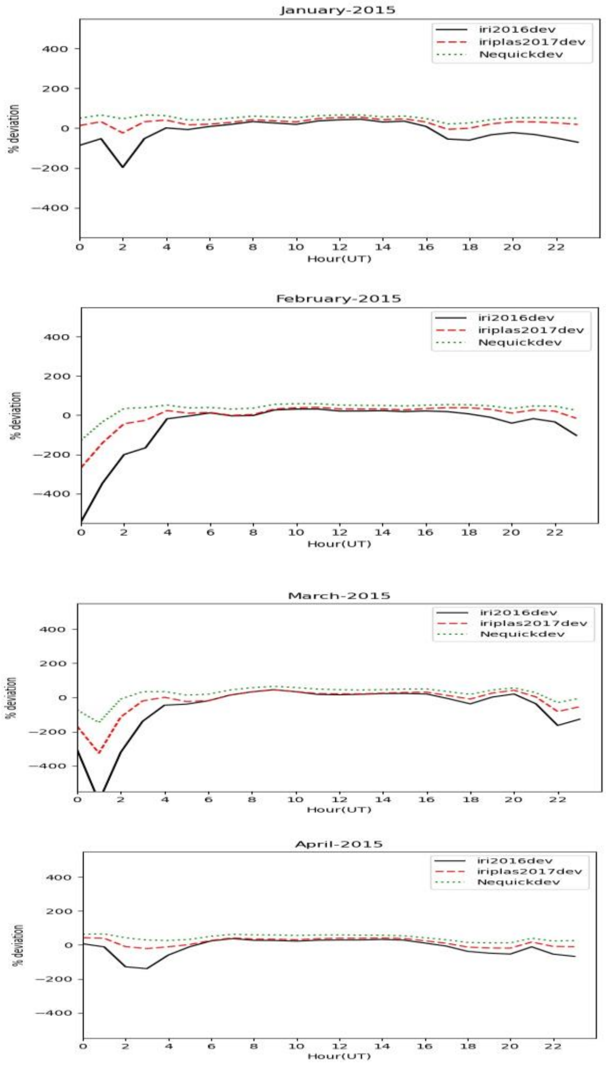

ISSN 2350-1030

International Journal of Recent Research in Physics and Chemical Sciences (IJRRPCS)
Vol. 10, Issue 2, pp: (13-40), Month: October 2023 – March 2024, Available at: www.paperpublications.org

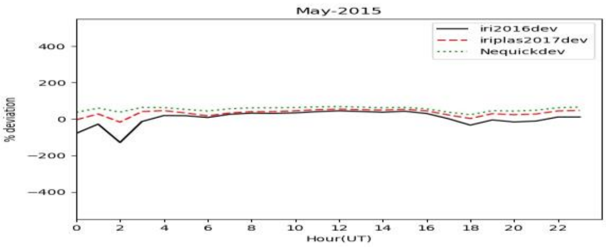

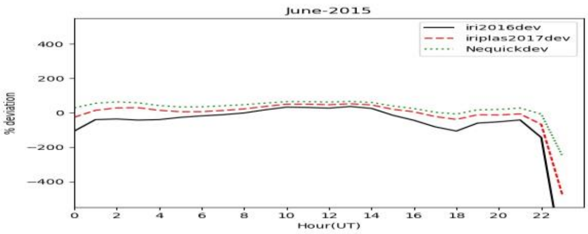

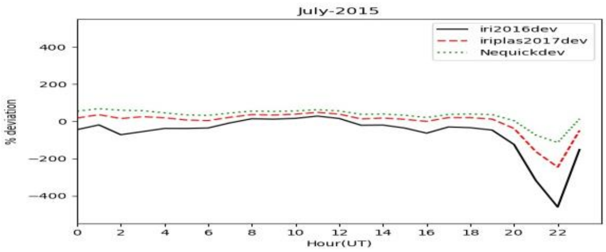

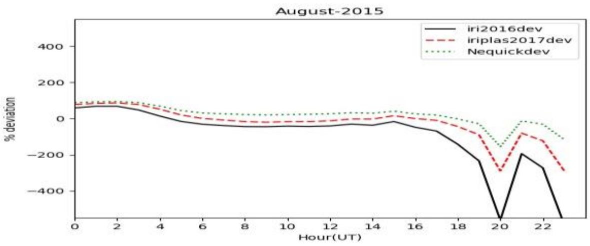

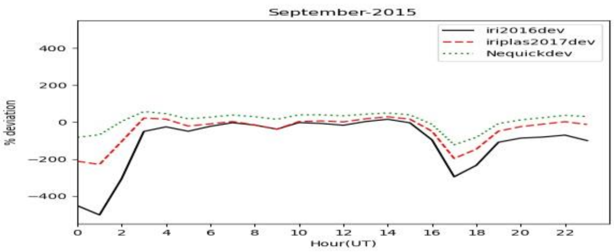

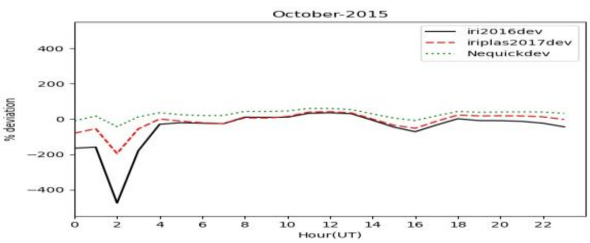

International Journal of Recent Research in Physics and Chemical Sciences (IJRRPCS)
Vol. 10, Issue 2, pp: (13-40), Month: October 2023 – March 2024, Available at: www.paperpublications.org

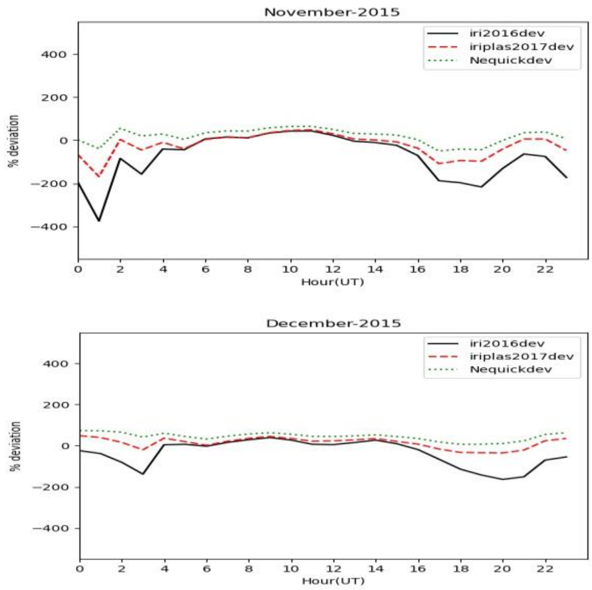

Fig. 9 Monthly Percentage Deviations of IRI-2016, IRI-Plas2017, and NeQuick models from GPS-TEC during the maximum phase

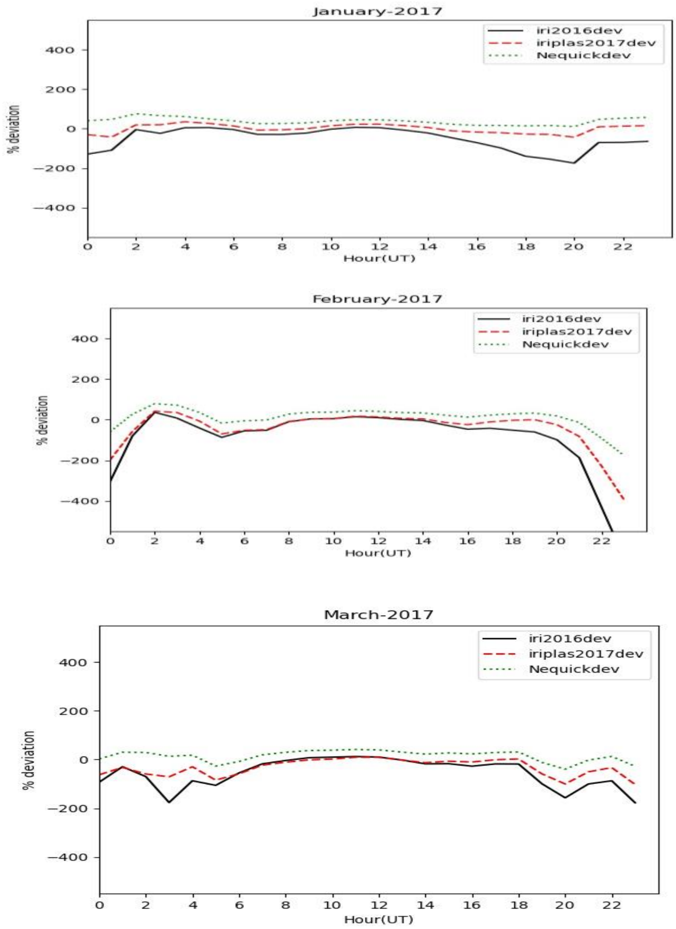

International Journal of Recent Research in Physics and Chemical Sciences (IJRRPCS)
Vol. 10, Issue 2, pp: (13-40), Month: October 2023 – March 2024, Available at: www.paperpublications.org

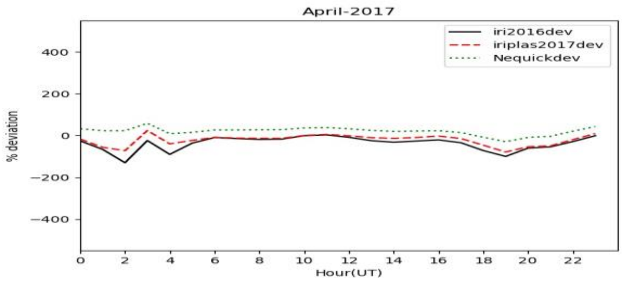

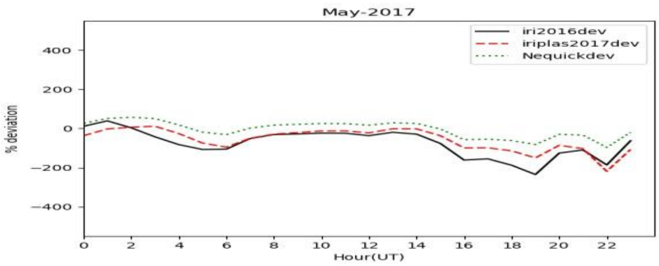

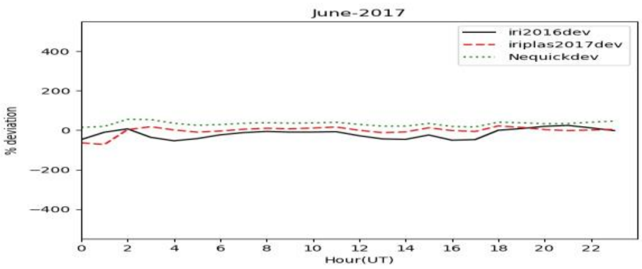

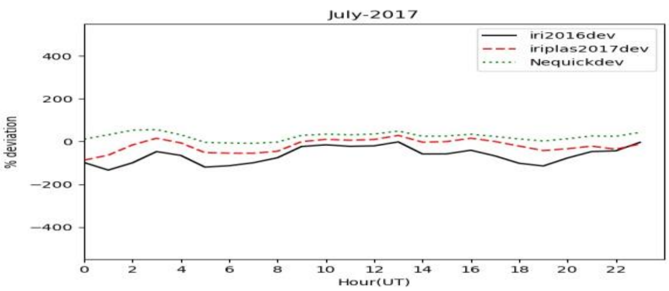

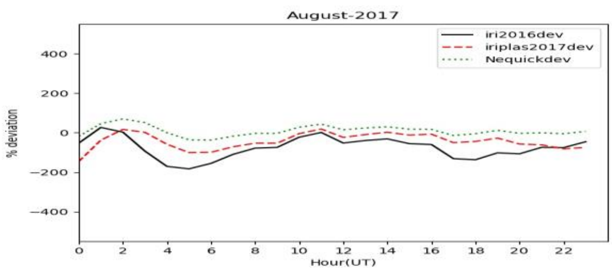

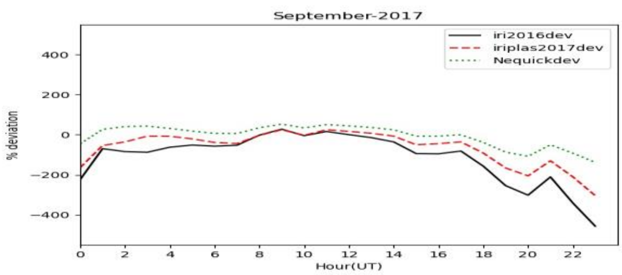

ISSN 2350-1030

International Journal of Recent Research in Physics and Chemical Sciences (IJRRPCS)
Vol. 10, Issue 2, pp: (13-40), Month: October 2023 – March 2024, Available at: www.paperpublications.org

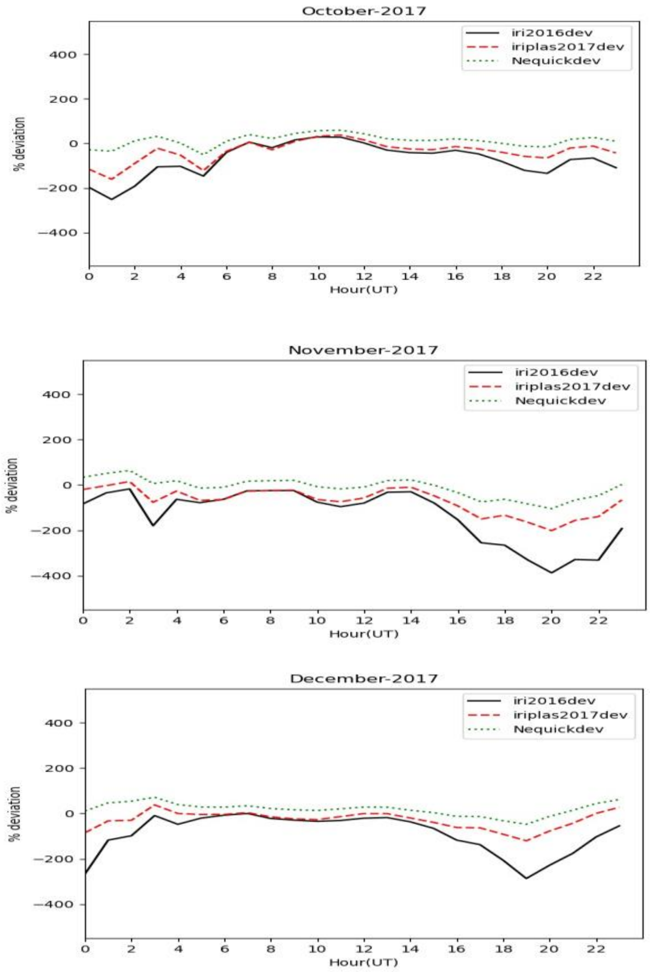

Fig. 10 Monthly Percentage Deviations of IRI-2016, IRI-Plas2017, and NeQuick models from GPS-TEC during the descending phase

Fig. 8-10 indicates the monthly percentage deviations of IRI-2016, IRI-Plas2017 and NeQuick-2 models from GPS-TEC during ascending, maximum and descending phases. On the figure lengend, iri2016dev, iriplas2017dev and Nequickdev denotes the deviations of IRI-2016, IRI-Plas2017 and NeQuick-2 models from GPS values. During the ascending phase, the IRI-2016 and IRI-Plas2017 models predictrions were good during the daytime between 06:00UT to 15:00UT hours of the day but their predictions were generally poor for all the months and they recorded overestimations of GPS-TEC during the early morning hours between (01:00T -05:00UT) and during the night hours between 16:00UT -24:00UT except the month of November where the IRI-Plas2017 model had the best performance. The NeQuick-2 model had the best perfornance between 15:00UT- 17:00UT hours of the day all throughout the months of the year except for the month of November where it had a worst performance and recorded underestimations of GPS-TEC during the day between 03:00UT-16:00UT and overestimations during the early morning hours (01:00UT-02:00UT) and night hours between (17:00UT-24:00UT). A very high deviations were observed during the months of August and October from the IRI-2016 model where its overestimations increases by 756% and 656% during the early morning hours of the day respectively. This is attributed to the absence of plasmapheric content input parameter in the models for these months [10], [63], [47]. Almost similar deviations were observed during the maximum and descending phases but with slight variations as were recorded during the ascending phase. Generally, the performances of models were good during the day time and poor during the early morning and night time hours.

ISSN 2350-1030

International Journal of Recent Research in Physics and Chemical Sciences (IJRRPCS)
Vol. 10, Issue 2, pp: (13-40), Month: October 2023 – March 2024, Available at: www.paperpublications.org

3.3 Anual Deviations of the IRI-2016, IRI-Plas2017, and NeQuick-2 from GPS-TEC

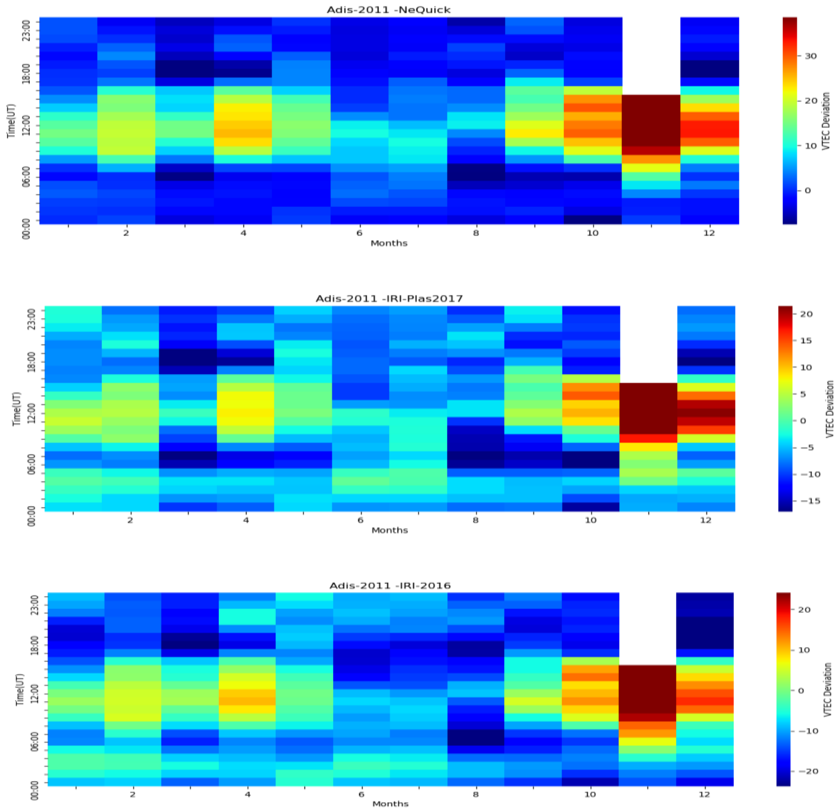

Fig. 11 Anual Deviations of the IRI-2016, IRI-Plas2017, and NeQuick-2 from GPS-TEC at ADIS for the year 2011

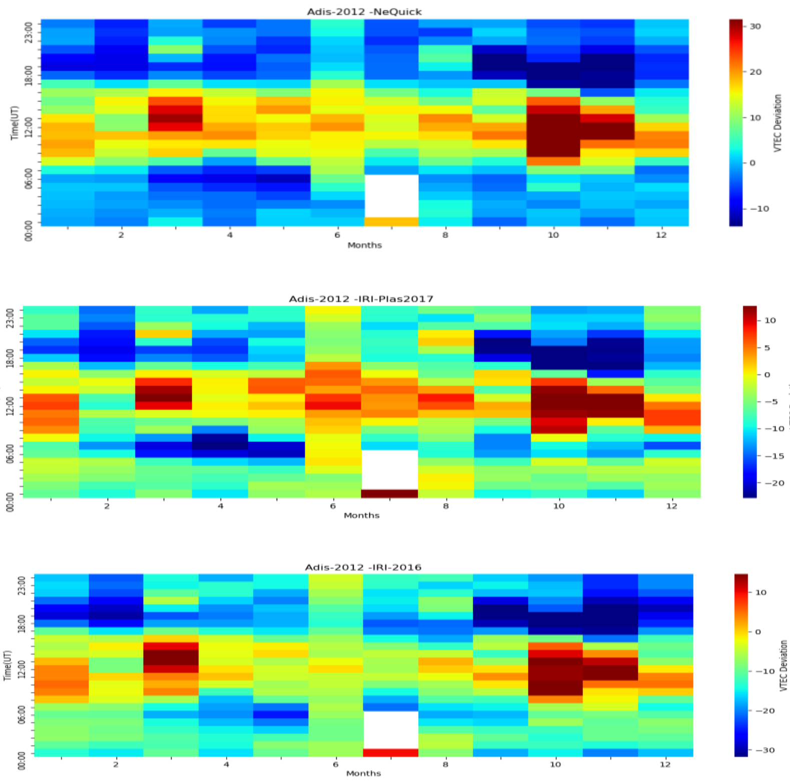

Fig. 12 Anual Deviations of the IRI-2016, IRI-Plas2017, and NeQuick from GPS-TEC at ADIS for the year 2012

ISSN 2350-1030

International Journal of Recent Research in Physics and Chemical Sciences (IJRRPCS)
Vol. 10, Issue 2, pp: (13-40), Month: October 2023 – March 2024, Available at: www.paperpublications.org

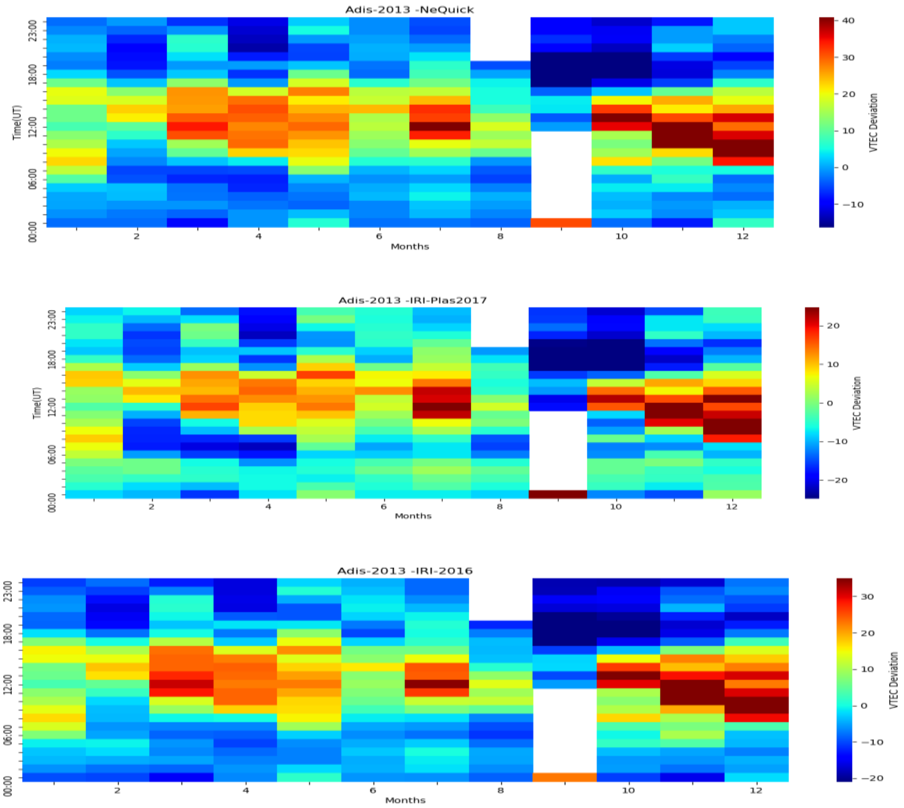

Fig. 13 Anual Deviations of the IRI-2016, IRI-Plas2017, and NeQuick from GPS-TEC at ADIS for the year 2013

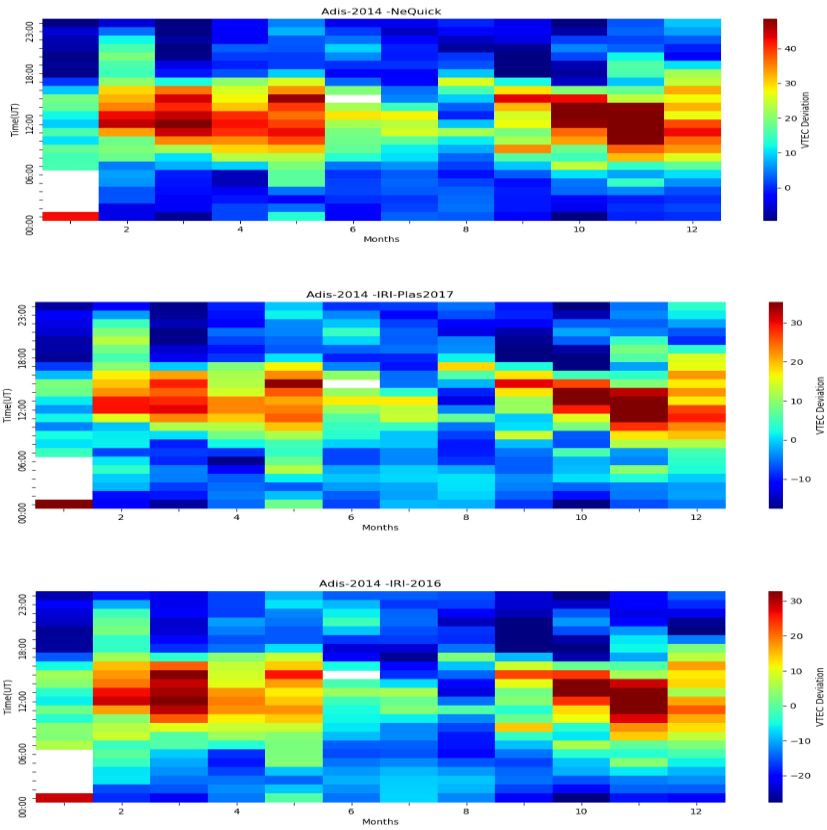

Fig. 14 Anual Deviations of the IRI-2016, IRI-Plas2017, and NeQuick from GPS-TEC at ADIS for the year 2014

International Journal of Recent Research in Physics and Chemical Sciences (IJRRPCS)
Vol. 10, Issue 2, pp: (13-40), Month: October 2023 – March 2024, Available at: www.paperpublications.org

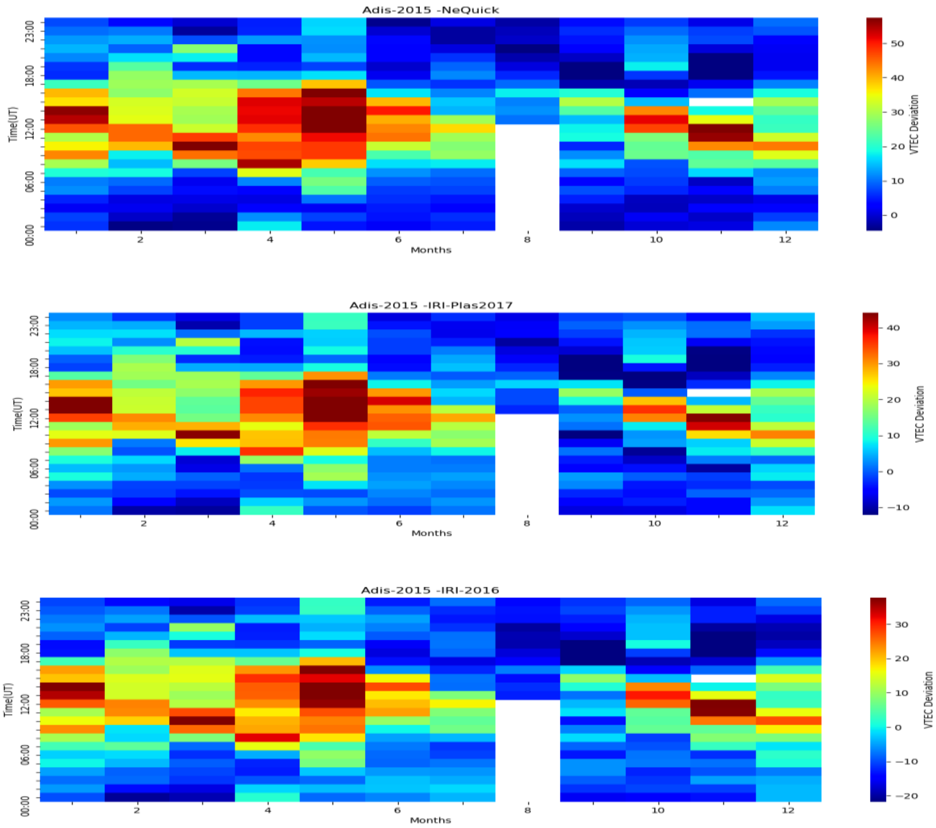

Fig. 15 Anual Deviations of the IRI-2016, IRI-Plas2017, and NeQuick from GPS-TEC at ADIS for the year 2015

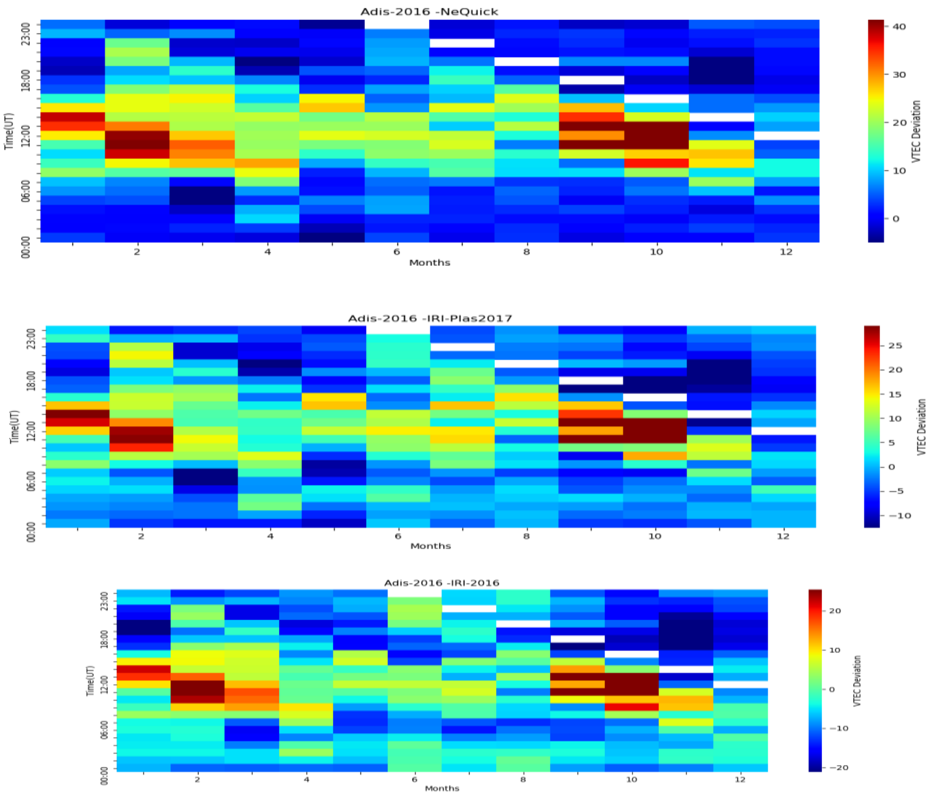

Fig. 16 Anual Deviations of the IRI-2016, IRI-Plas2017, and NeQuick from GPS-TEC at ADIS for the year 2016

International Journal of Recent Research in Physics and Chemical Sciences (IJRRPCS)
Vol. 10, Issue 2, pp: (13-40), Month: October 2023 – March 2024, Available at: www.paperpublications.org

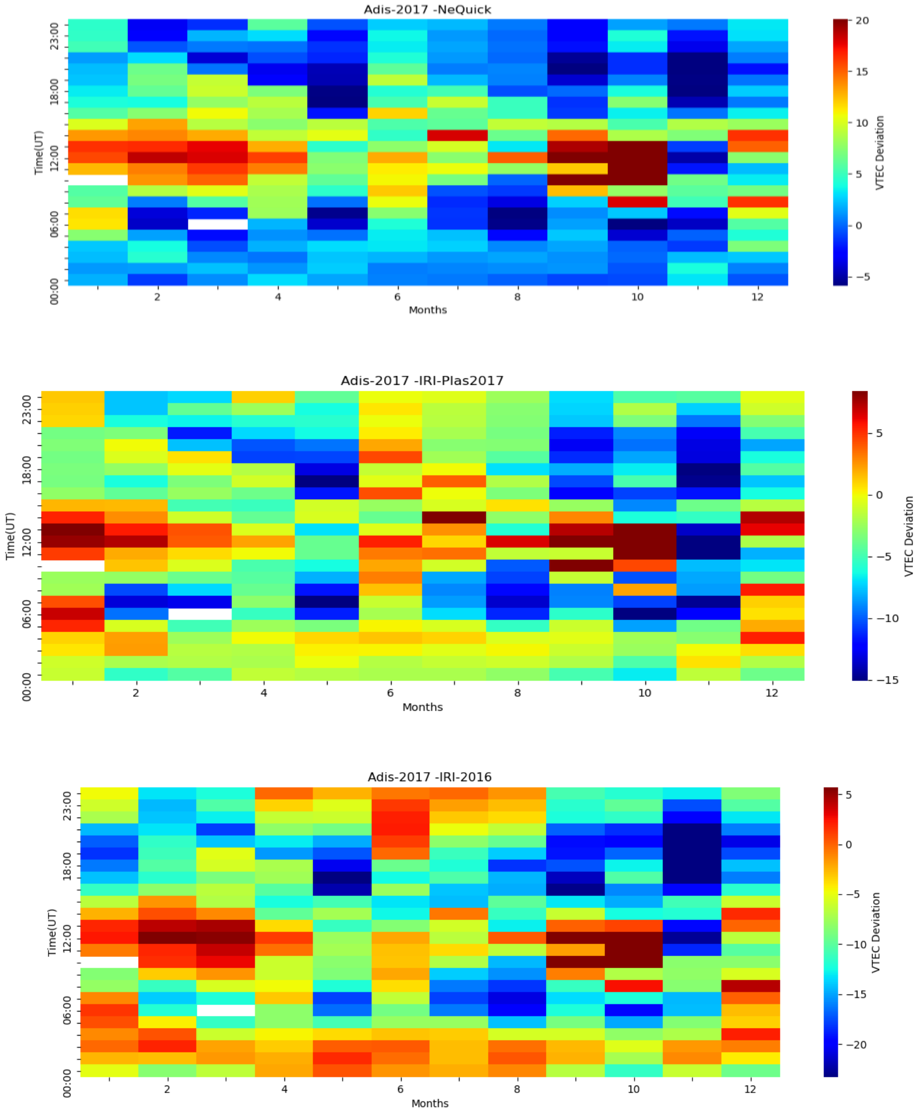

Fig. 17 Anual Deviations of the IRI-2016, IRI-Plas2017, and NeQuick from GPS-TEC at ADIS for the year 2017

Fig. 11-17 illustrates the annual deviation of IRI-2016, IRI-Plas2017 and NeQuick-2 models from GPS-TEC at ADIS from 2011 to 2017. From Fig. 15- 21, brownish red color indicates slight overestimations of GPS-TEC by IRI-2016, IRI-Plas2017 and NeQuick-2 models which invariably indicates a fair performance of the model, while the brown color indicates very high overestimations of GPS-TEC data thus, a worst performance of the model. The yellow color denotes no deviation of IRI-2016, IRI-Plas2017 and NeQuick-2 models from GPS-TEC hence, best performance. The light blue color indicates a slight underestimation (fair performance of the model), while dark blue color shows a highest underestimations (poor performance of the model). The white patches from the mass plots indicates that no data were recorded during that time of the day. The highest during of missing data recorded was during 2015 from 24:00UT to 13:00UT in the month of August. In 2011, data were not recorded for 7hours (16:00UT-23:00T) in November. The same during of missing data were recorded in 2012 and 2014 between 02:00UT and 07:00UT in July and January respectively. The year 2013 recorded missing data in two different consecutive months (August and September) from 20:00UT to 23:00UT and 02:00UT to 12:00UT respectively. The year 2017 recorded the highest avalaibilty of data. From this analysis, we confirm that the IRI-Plas2017 model had the best performance from 2011 to 2017 except for year 2015 where the IRI-2016 and IRI-Plas2017 models had exactly the same level of performance as reported in the work of [87].

International Journal of Recent Research in Physics and Chemical Sciences (IJRRPCS)
Vol. 10, Issue 2, pp: (13-40), Month: October 2023 – March 2024, Available at: www.paperpublications.org

3.4 Annual Root Mean Square Error for IRI-2016, IRI-Plas2017 and NeQuick-2 models

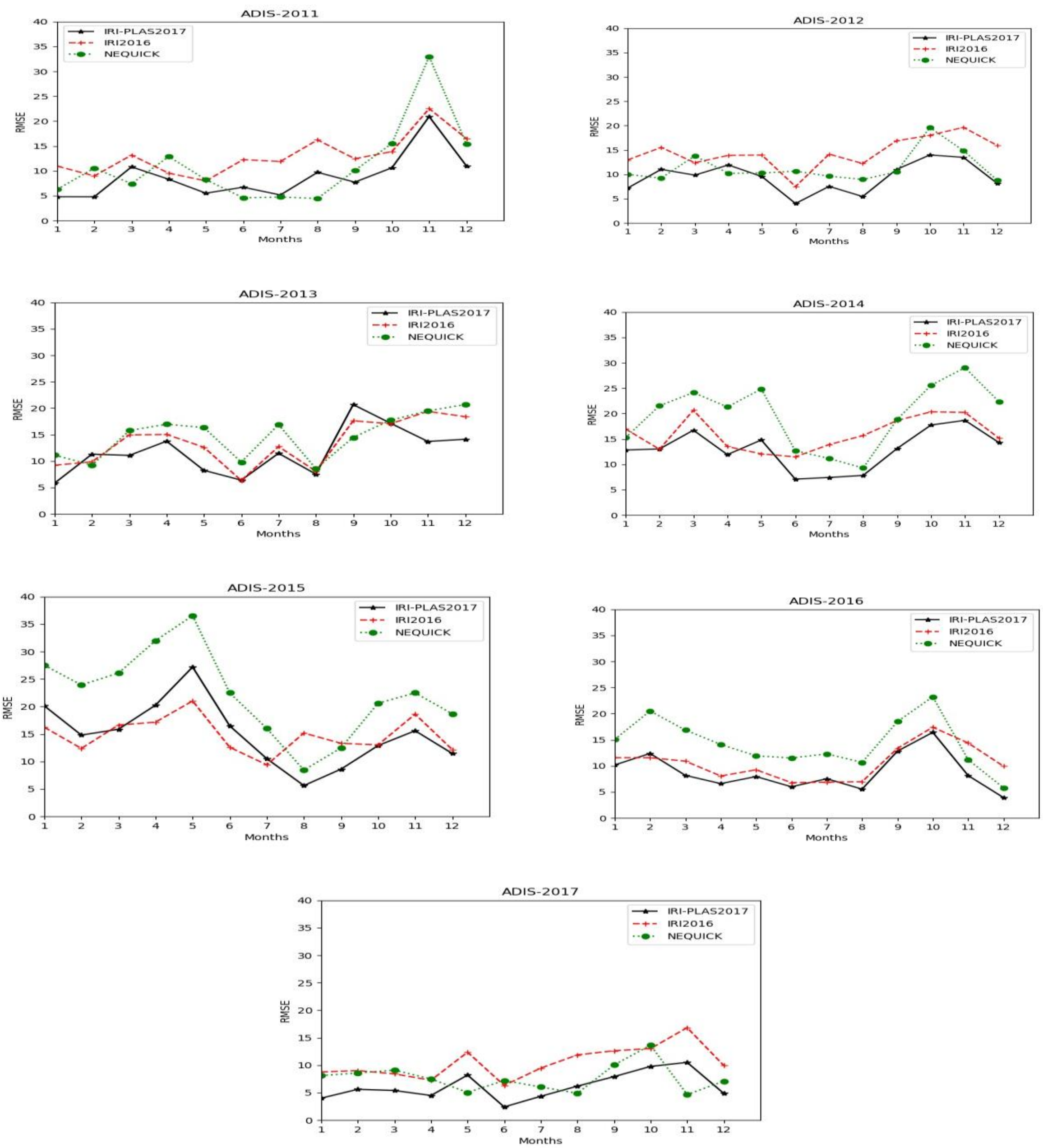

Fig. 18 Annual Root Mean Square Error for IRI-2016, IRI-Plas2017 and NeQuick models at ADIS from 2011-2017

Fig. 18 shows the annual Root Mean Square Error (RMSE) for IRI-2016, IRI-Plas2017 and NeQuick-2 models at ADIS from 2011 to 2017. In the year 2011, the IRI-Plas2017 model had the lowest RMSE value throughout the months of the year except in the month of June, July and August where the NeQuick-2 model recorded recorded the lowest RMSE values. In the month of November, the performance of the IRI-Plas2017 model was worst with a value recorded as ~21 TECU which was the highest value recorded from any model all through out the year. Almost similar features were recorded from 2012 to 2014 except in 2013 where the highest RMSE value shifted to the month of December from the NeQuick-2 model. In the year 2015, the highest value from the RMSE analysis was still recorded from the NeQuick-2 model in the month of May with a value of ~37 TECU but in 2016, the highest RMSE from the NeQuick-2 model shifted again to the month of October. Lastly, the year 2017 had a change in the highest value of RMSE recorded. This year, the highest RMSE recorded ~17 TECU from the IRI-2016 model while the least RMSE was recorded during the month of June with ~3 TECU as it value.

ISSN 2350-1030

International Journal of Recent Research in Physics and Chemical Sciences (IJRRPCS)
Vol. 10, Issue 2, pp: (13-40), Month: October 2023 – March 2024, Available at: www.paperpublications.org

3.5 Annual Root Mean Square Error for IRI-2016, IRI-Plas2017 and NeQuick-2 models

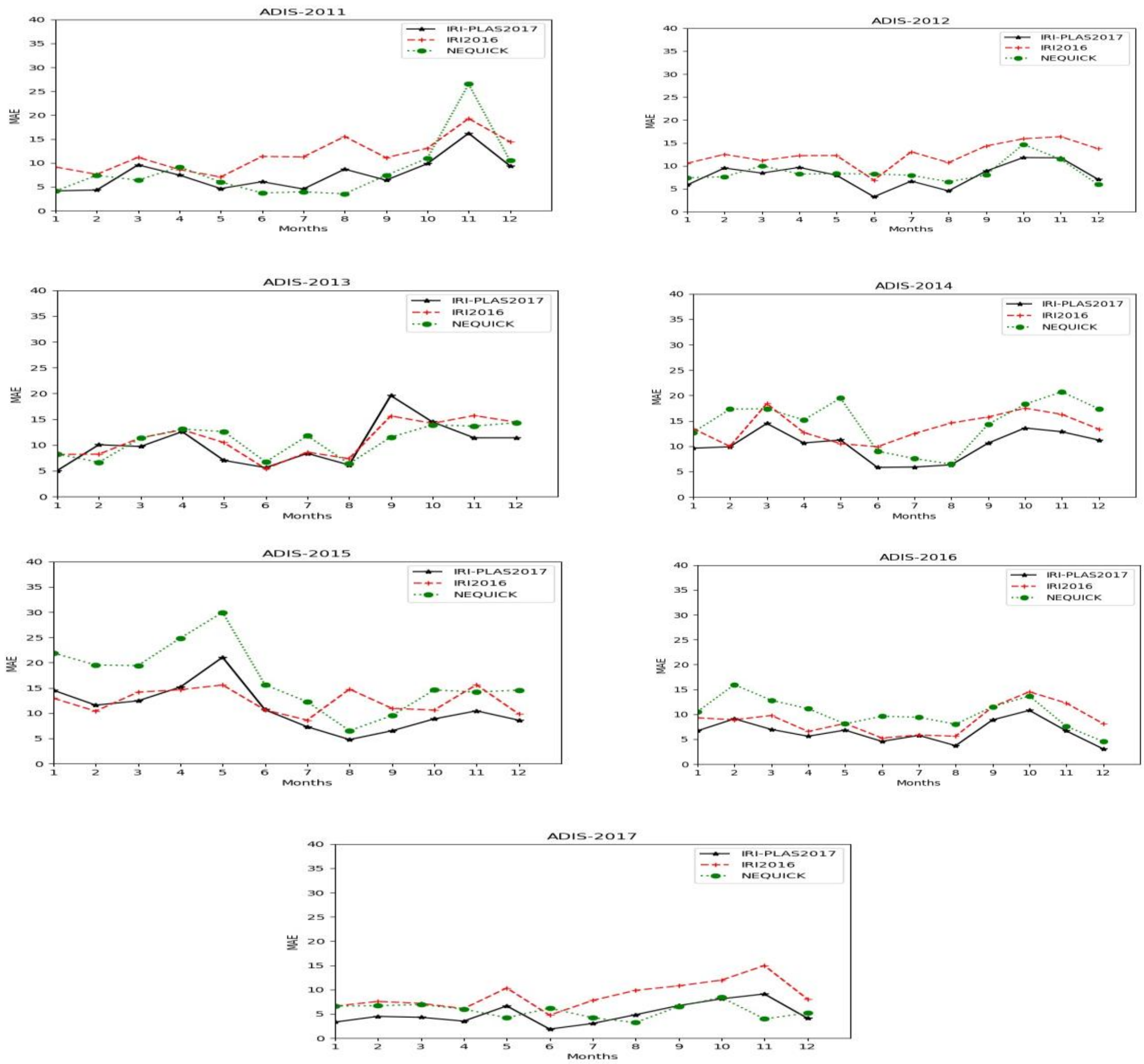

Fig. 19 Annual Mean Absolute Error for IRI-2016, IRI-Plas2017 and NeQuick models at ADIS from 2011-2017

Fig. 19 depicts the annual Mean Absolute Error (MAE) for IRI-2016, IRI-Plas2017 and NeQuick-2 models at ADIS from 2011 to 2017. The MAE is employed to further investigate the degree of deviations of the IRI-2016, IRI-Plas2017 and NeQuick-2 models from GPS-TEC and in the same vain to show the level of their performance. From our results, we concluded that MAE values were ~3 TECU lower than the RMSE in all the solar cycle phases. Also, from the results presented here, we affirm that MAE can better assess the performance of a model than RMSE. Our affirmation was in agreement with the work of [29].

Table 3: The Annual performance of IRI-Plas2017, IRI-2016, and NeQuick at ADIS

S/N	YEAR	IRI-Plas2017	IRI-2016	NeQUICK
1	2011	62.7%	4.2%	33.1%
2	2012	75%	5%	20%
3	2013	66.7%	16.7%	16.6%
4	2014	81.3%	16.2%	2.5%
5	2015	48%	48%	4%
6	2016	81.3%	16.2%	2.5%
7	2017	72%	5%	23%

International Journal of Recent Research in Physics and Chemical Sciences (IJRRPCS)
Vol. 10, Issue 2, pp: (13-40), Month: October 2023 – March 2024, Available at: www.paperpublications.org

The percentage performance of IRI-Plas2017, IRI-2016 and NeQuick-2 models in all the months for 7 years at ADIS in the east African region is shown in table 3. The table clearly indicates that IRI-Plas2017 model had the best performances in all the months from 2011 to 2017 over the IRI-2016 and NeQuick-2 models. It also clearly depicts that the IRI-Plas2017 model had its best performance of 81.3% in 2016 while the NeQuick-2 had the worst performance of 2.5% in the same year.

4. CONCLUSIONS

In this present study, we have analyzed the performance of IRI-2016, IRI-Plas2017, and NeQuick-2 models using GPS-TEC data in the East African low latitude region (Addis Ababa) during solar cycle 24 (2011-2017). We affirmed that the lowest TEC values (as low as ~2 TECU from the NeQuick-2 model) were recorded around the post-midnight period (02:00UT) while the highest values (as high as ~85 TECU from GPS-TEC) of TEC were recorded around the pre-noon period (11:00UT). Seasonally, we infer that equinoxes recorded higher values of TEC than solstice seasons but seasonal/winter anomaly were encountered by the TEC values in all the phases of the solar cycle except during the descending phase. Nighttime enhancement is more pronounced and stronger during the ascending phase and weakest during the descending phase Also from our results, MAE gives values ~3 TECU lower than those of the RMSE. From the results of our statistically analysis, we deduced that the IRI-Plas2017 model had the best performance of 71.4% of the months while the IRI-2016 and NeQuick-2 model had same performance of 14.3% each of the months under consideration. Conclusively, IRI-Plas2017 model predicts TEC better than the IRI-2016 and NeQuick-2 models in the East African region. The poor performance of IRI-2016 model from this research work has proven that NeQuick topside option of the model (IRI-2016) is accurate and better in predicting TEC in the East African region than the IRI-2001 topside option as reported by [10]. Also, the low predictive power of the NeQuick-2 model is as a result of low data input into the model during its validation process.

ACKNOWLEGDEMENTS

The Authors thank Krishma Gopi Seemala for making the GOPI_TEC processing software available on (https://seemala.blogspot.com) and they are also grateful to the University NAVSTAR Consortium (UNAVCO) for making the GPS-TEC data available on their website at http://www.unavco.org

Authors Contributions

Y.O.K, E.O, and O.O analyzed data, plotted the figures and wrote the initial manuscript. S.A.O and A.S.A wrote part of the methodology while R.B.A and R.A.A proof read and corrected the entire grammatical arrangements of the manuscript.

Conflicts of Interest

The Authors declare no conflict or competing interest

REFERENCES

[1] Abdu, M. A.: Equatorial ionosphere–thermosphere system: Electrodynamics and irregularities. Advances in Space Research, 35(5), 771-787 (2005).

[2] Adebesin, B. O., Ikubanni, S. O., Adebiyi, S. J., Bakare, N. O., Okoh, D. I., Adeniyi, J. O., Adekoya, B. J.: Pattern of F2-layer peak electron density across African Ionosonde locations and response to solar activity. Advances in Space Research, 72(3), 884-896 (2023).

[3] Adekoya, B. J., Chukwuma, V. U., Adebiyi, S. J., Adebesin, B. O., Ikubanni, S. O., Bolaji, O. S., Bisuga, O. O.: Ionospheric storm effects in the EIA region in the American and Asian-Australian sectors during geomagnetic storms of October 2016 and September 2017. Advances in Space Research (2023). https://doi.org/10.1016/j.asr.2023.04.016.

[4] Adewale, A.O., Migoya, Y.O., Oyeyemi, E.O.: Assessment of NeQuick Model at Lagos, Nigeria using GPS TEC. Unilag Journal of Medicine, Sci and Tech. 1, 1-14. (2013).

[5] Adewale, A.O., Oyeyemi, E.O., Adeniyi, J.O., Adeloye, A.B., Oladapo, O.A.: Comparison of total electron content predicted using the IRI-2007 model with GPS observations over Lagos, Nigeria. Indian journal of radio and space physics 40, 21-25 (2011).

[6] Afraimovich, E. L., Astafyeva, E. I., Demyanov, V. V., Edemskiy, I. K., Gavrilyuk, N. S., Ishin, A. B., Zhivetiev, I. V.: A review of GPS/GLONASS studies of the ionospheric response to natural and anthropogenic processes and phenomena. Journal of Space Weather and Space Climate, 3, A27 (2013).

[7] Aggarwal, M.: TEC variability near northern EIA crest and comparison with IRI model. Advances in space research, 48(7), 1221-1231(2011).

[8] Ahoua, S. M., Habarulema, J. B., Obrou, O. K., Cilliers, P. J., Zaka, Z. K.: Evaluation of the NeQuick model performance under different geomagnetic conditions over South Africa during the ascending phase of the solar cycle (2009–2012). In *Annales Geophysicae* (Vol. 36, No. 5, pp. 1161-1170). Göttingen, Germany: Copernicus Publications (2018).

[9] Akala, A. O., Oyeyemi, E. O., Amaechi, P. O., Radicella, S. M., Nava, B., & Amory-Mazaudier, C.: Longitudinal responses of the equatorial/low-latitude ionosphere over the oceanic regions to geomagnetic storms of May and September 2017. Journal of Geophysical Research: Space Physics, 125(8) (2020), e2020JA027963.

[10] Akala, A. O., Somoye, E. O., Adewale, A. O., Ojutalayo, E. W., Karia, S. P., Idolor, R. O., Doherty, P. H.: Comparison of GPS-TEC observations over Addis Ababa with IRI-2012 model predictions during 2010–2013. *Advances in Space Research*, *56*(8), 1686-1698 (2015).

[11] Alcay, S., Oztan, G., Selvi, H. Z.: Comparison of IRI_PLAS and IRI_2012 model predictions with GPS-TEC measurements in different latitude regions. Annals of Geophysics, 60(5), 0549 (2017).

[12] Alluri, V., Rajesh, V. R., Joshi, S., Baneerje, S., Kothari, N.: Comparison and Validation of VTEC Derived from GPS, IRI-Plas and NeQuick-2 During 2015 and 2019 in India. International Journal of Geoinformatics, 16(4), 58-70 (2020).

[13] Ambili, K. M., Choudhary, R. K.: On the impact of meridional wind circulation changes in the electron density distribution over the Indian equatorial and low latitude ionospheric region during a severe geomagnetic storm. Advances in Space Research, 70(7), 2058-2069 (2022).

[14] Ameen, M. A., Jabbar, M. A., YU, X., Zhen, W., Murtaza, G., Chishtie, F.,Atiq, M.: Comparison of Ionospheric Total Electron Content (TEC) over Sonmiani (Pakistan) with NeQuick-2 and IRI-2012 during July 2014 - June 2015. Advances in Space Research (2018). doi:10.1016/j.asr.2018.09.017.

[15] Ansari, K., Corumluoglu, O., Panda, S. K.: Analysis of ionospheric TEC from GNSS observables over the Turkish region and predictability of IRI and SPIM models. Astrophysics and Space Science, 362(4), 65 (2017).

[16] Atici, R.: Comparison of GPS TEC with modelled values from IRI 2016 and IRI-PLAS over Istanbul, Turkey. Astrophysics Space Sci , 363:231 (2018).

[17] Balan, N., Bailey, G. J., Nair, R. B., Titheridge, J. E.: Nighttime enhancements in ionospheric electron content in the northern and southern hemispheres. Journal of atmospheric and terrestrial physics, 56(1), 67-79 (1994).

[18] Bhattacharya, S., Purohit, P. K., Gwal, A. K.: Ionospheric time delay variations in the equatorial anomaly region during low solar activity using GPS. 94.20. dt; 92.70. Qr (2009).

[19] Bhattacharyya, A.: Equatorial plasma bubbles: A review. Atmosphere, 13(10), 1637 (2022).

[20] Bidaine, B., Prieto-Cerdeira, R., Orus, R.: NeQuick: In-Depth Analysis and New Developments. Ann. Geophysics 48, 491-495 (2006).

[21] Bilitza, D., Altadill, D., Truhlik, V., Shubin, V., Galkin, I., Reinisch, B., Huang, X.: International Reference Ionosphere 2016: From ionospheric climate to real-time weather predictions. Space weather, 15(2), 418-429 (2017).

[22] Bilitza, D., Reinisch, B. W., Radicella, S. M., Pulinets, S., Gulyaeva, T., Triskova, L.: Improvements of the International Reference Ionosphere model for the topside electron density profile. Radio science, 41(05), 1-8 (2006).

[23] Bilitza, D., Reinisch, B. W.: International reference ionosphere 2007: Improvements and new parameters. Advances in space research, 42(4), 599-609 (2008).

[24] Bilitza, D.: A correction for the IRI topside electron density model based on Alouette/ISIS topside sounder data. Advances in Space Research, 33(6), 838-843 (2004).

[25] Bilitza, D.: The International Reference Ionosphere: Rawer's IRI and its status today. Adv.Radio Sci. 12, 231–236 (2014).

[26] Bolaji, O.S., Oyeyemi, E.O., Adewale, A.O., Wu, Q., Okoh, D., Doherty, P.H., Kaka, R.O., Abbas, M., Owolabi, C., Jidele, P.A.: Assessment of IRI-2012, NeQuick-2 and IRI-Plas 2015 models with observed equatorial ionization anomaly in Africa during 2009 sudden stratospheric warming event. Journal of Atmospheric and Solar-Terrestrial Physics 164,203–214 (2017).

[27] Brahmanandam, P. S., Uma, G., Liu, J. Y., Chu, Y. H., Latha Devi, N. S. M. P., Kakinami, Y.: Global S4 index variations observed using FORMOSAT-3/COSMIC GPS RO technique during a solar minimum year. Journal of Geophysical Research: Space Physics, 117(A9) (2012).

[28] Cander, L.R:. Ionospheric research and space weather services. Journal of atmospheric and solar-terrestrial physics, 70(15), 1870-1878 (2008).

[29] Chai, T., Draxler, R. R.: Root mean square error (RMSE) or mean absolute error (MAE)?–Arguments against avoiding RMSE in the literature. Geoscientific model development, 7(3), 1247-1250 (2014).

[30] Chakraborty, S., Ray, S., Sur, D., Datta, A., Paul, A.: Effects of CME and CIR induced geomagnetic storms on low-latitude ionization over Indian longitudes in terms of neutral dynamics. Advances in Space Research, 65(1), 198-213(2020).

[31] Chekole, D. A., Giday, N. M., Nigussie, M.: Performance of NeQuick-2, IRI-Plas 2017 and GIM models over Ethiopia during varying solar activity periods. Journal of Atmospheric and Solar-Terrestrial Physics, 195, 105117 (2019). doi:10.1016/j.jastp.2019.105117.

[32] Chen, J., Ren, X., Zhang, X., Zhang, J., Huang, L.: Assessment and validation of three ionospheric models (IRI-2016, NeQuick2 and IGS-GIM) from 2002 to 2018. Space Weather. (2020). doi:10.1029/2019sw002422.

[33] Chen, Y., Liu, L., Le, H., Wan, W., Zhang, H.: The global distribution of the dusk-to-nighttime enhancement of summer NmF2 at solar minimum. Journal of Geophysical Research: Space Physics, 121(8), 7914-7922 (2016).

[34] Chen, Y., Liu, L., Le, H., Zhang, H.: Equatorial north-south difference of noontime electron density bite-out in the F2 layer. Journal of Geophysical Research: Space Physics, 125(8), (2020). e2020JA028124.

[35] Chen, Y., Liu, L., Le, H., Zhang, H.: Latitudinal Dependence of Daytime Electron Density Bite-Out in the Ionospheric F2-Layer. Journal of Geophysical Research: Space Physics, 126(1), (2021). e2020JA028277.

[36] Cheng, K., Huang, Y. N.: Comparing the IRI prediction with the observed equatorial anomaly in the Total Electron Content around 120° E longitude. Advances in Space Research, 18(6), 249-258 (1996).

[37] Cooper, C., Mitchell, C. N., Wright, C. J., Jackson, D. R., Witvliet, B. A.: Measurement of ionospheric total electron content using single-frequency geostationary satellite observations. Radio Science, 54(1), 10-19 (2019).

[38] Coster, A., Komjathy, A.: Space weather and the global positioning system. Space Weather, 6(6) (2008).

[39] Dabas, R. S., Singh, L., Lakshmi, D. R., Subramanyam, P., Chopra, P., Garg, S. C.: Evolution and dynamics of equatorial plasma bubbles: Relationships to ExB drift, postsunset total electron content enhancements, and equatorial electrojet strength. Radio Science, 38(4), 14-1 (2003).

[40] Dashora, N., Suresh, S.: Characteristics of low-latitude TEC during solar cycles 23 and 24 using global ionospheric maps (GIMs) over Indian sector. Journal of Geophysical Research: Space Physics, 120(6), 5176-5193 (2015).

[41] Datta-Barua, S., Doherty, P. H., Delay, S. H., Dehel, T., Klobuchar, J. A.: Ionospheric scintillation effects on single and dual frequency GPS positioning. In Proceedings of the 16th international technical meeting of the satellite division of the institute of navigation (ION GPS/GNSS 2003) (pp. 336-346) (2003).

[42] de Dieu Nibigira, J., Sivavaraprasad, G., Ratnam, D. V.: Performance analysis of IRI-2016 model TEC predictions over Northern and Southern Hemispheric IGS stations during descending phase of solar cycle 24. Acta Geophysica, 69(4), 1509-1527 (2021).

[43] Dugassa, T., Habarulema, J. B., Nigussie, M.: Statistical study of geomagnetic storm effects on the occurrence of ionospheric irregularities over equatorial/low-latitude region of Africa from 2001 to 2017. Journal of Atmospheric and Solar-Terrestrial Physics, 199, 105198. (2020).

[44] Eyelade, V. A., Adewale, A. O., Akala, A. O., Bolaji, O. S., Rabiu, A. B.: Studying the variability in the diurnal and seasonal variations in GPS total electron content over Nigeria. In Annales Geophysicae (Vol. 35, No. 3, pp. 701-710). Copernicus GmbH (2017).

[45] Ezquer, R. G., Scida, L. A., Orué, Y. M., Nava, B., Cabrera, M. A., Brunini, C.: NeQuick 2 and IRI Plas VTEC predictions for low latitude and South American sector. Advances in Space Research, 61(7), 1803-1818 (2018).

[46] Fedrizzi, M., de Paula, E. R., Kantor, I. J., Langley, R. B., Santos, M. C., Komjathy, A.: Mapping the low-latitude ionosphere with GPS. GPS WORLD, 13(2), 41-47 (2002).

[47] Forootan, E., Kosary, M., Farzaneh, S., Schumacher, M.: Empirical Data Assimilation for Merging Total Electron Content Data with Empirical and Physical Models. *Surveys in Geophysics*, 1-31 (2023).

[48] Fridman, S. V., Nickisch, L. J., Aiello, M., Hausman, M.: Real-time reconstruction of the three-dimensional ionosphere using data from a network of GPS receivers. Radio science, 41(05), 1-7(2006).

[49] Fu, S., Zhang, X., Zhao, L., Li, Y.: Variations of the galactic cosmic rays in the recent solar cycles. The Astrophysical Journal Supplement Series, 254(2), 37. (2021).

[50] Galkin, I., Froń, A., Reinisch, B., Hernández-Pajares, M., Krankowski, A., Nava, B., Batista, I.: Global monitoring of ionospheric weather by GIRO and GNSS data fusion. Atmosphere, 13(3), 371. (2022).

[51] Gasperini, F., Crowley, G., Immel, T. J., Harding, B. J.: Vertical wave coupling in the low-latitude Ionosphere-Thermosphere as revealed by concurrent ICON and COSMIC-2 Observations. Space Science Reviews, 218(7), 55. (2022).

[52] Ghodpage, R. N., Patil, P. T., Gurav, O. B., Gurubaran, S., Sharma, A. K.: Ionospheric response to major storm of 17th March 2015 using multi-instrument data over low latitude station Kolhapur (16.8 N, 74.2 E, 10.6 dip. Lat.). Advances in Space Research, 62(3), 624-637 (2018).

[53] Hazarika, A., Bhuyan, K., Kalita, B. R., Bhuyan, P. K., Borgohain, A., Tiwari, R. C.: Performance evaluation of IRI, IRI Plas and SAMI2 during the consecutive prolonged solar minimum of cycles 23 and 24 around 100° E. Advances in Space Research (2023).

[54] Hoque, M. M., Jakowski, N.: Higher order ionospheric propagation effects on GPS radio occultation signals. Advances in space research, 46(2), 162-173. (2010).

[55] Jakowski, N., Heise, S., Wehrenpfennig, A., Schlüter, S., Reimer, R.: GPS/GLONASS-based TEC measurements as a contributor for space weather forecast. Journal of Atmospheric and Solar-Terrestrial Physics, 64(5-6), 729-735. (2002).

[56] Jakowski, N., Mayer, C., Hoque, M. M., Wilken, V.: Total electron content models and their use in ionosphere monitoring. Radio Science, 46(06), 1-11 (2011).

[57] Jee, G., Burns, A. G., Kim, Y. H., Wang, W.: Seasonal and solar activity variations of the Weddell Sea Anomaly observed in the TOPEX total electron content measurements. Journal of Geophysical Research: Space Physics, 114(A4). (2009).

[58] Jiang, C., Wang, W., Yang, G., Zhao, Z.: A numerical study of noontime bite-outs in F2-region electron density. Advances in Space Research, 71(3), 1818-1826 (2023).

[59] Joshua, B. W., Adeniyi, J. O., Olawepo, A. O., Rabiu, B., Daniel, O., Adebiyi, S. J., Abdurahim, B.: Latitudinal dependence of ionospheric responses to some geomagnetic storms during low solar activity. Geomagnetism and Aeronomy, 61, 418-437 (2021).

[60] Katsavrias, C., Aminalragia-Giamini, S., Papadimitriou, C., Daglis, I. A., Sandberg, I., Jiggens, P.: Radiation belt model including semi-annual variation and solar driving (sentinel). Space Weather, 20(1), (2022). e2021SW002936.

[61] Kenpankho, P., Watthanasangmechai, K., Supnithi, P., Tsugawa, T., Maruyama, T.: Comparison of GPS TEC measurements with IRI TEC prediction at the equatorial latitude station, Chumphon, Thailand. Earth, planets and space, 63(4), 365-370 (2011).

[62] Kintner, P. M., Ledvina, B. M.: The ionosphere, radio navigation, and global navigation satellite systems. Advances in Space Research, 35(5), 788-811 (2005).

[63] Klimenko, M. V., Klimenko, V. V., Zakharenkova, I. E., Cherniak, I. V.: The global morphology of the plasmaspheric electron content during Northern winter 2009 based on GPS/COSMIC observation and GSM TIP model results. Advances in Space Research, 55(8), 2077–2085 (2015). doi:10.1016/j.asr.2014.06.027.

[64] Kumar, A., Ramsankaran, R. A. A. J., Brocca, L., Muñoz-Arriola, F.: A simple machine learning approach to model real-time streamflow using satellite inputs: Demonstration in a data scarce catchment. Journal of Hydrology, 595, 126046 (2021).

[65] Kutiev, I., Tsagouri, I., Perrone, L., Pancheva, D., Mukhtarov, P., Mikhailov, A., Torta, J. M.: Solar activity impact on the Earth's upper atmosphere. Journal of Space Weather and Space Climate, 3, A06 (2013).

[66] Lazzús, J. A., Salfate, I., Vega-Jorquera, P.: Intense Geomagnetic Storms in The Maximum Phase of Solar Cycle 24 Observed From a Low-Latitude Ground Station. Geofísica internacional, 61(4), 267-286 (2022).

[67] Lee, W. K., Kil, H., Kwak, Y. S., Wu, Q., Cho, S., Park, J. U.: The winter anomaly in the middle-latitude F region during the solar minimum period observed by the Constellation Observing System for Meteorology, Ionosphere, and Climate. Journal of Geophysical Research: Space Physics, 116(A2) (2011).

[68] Li, Q., Hao, Y., Zhang, D., Xiao, Z.: Nighttime enhancements in the midlatitude ionosphere and their relation to the plasmasphere. Journal of Geophysical Research: Space Physics, 123(9), 7686-7696 (2018).

[69] Li, Q., Liu, L., He, M., Huang, H., Zhong, J., Yang, N., Cui, J.: A global empirical model of electron density profile in the F region ionosphere basing on COSMIC measurements. Space Weather, 19(4), e2020SW002642 (2021).

[70] Liu, H., Stolle, C., Förster, M., & Watanabe, S.: Solar activity dependence of the electron density in the equatorial anomaly regions observed by CHAMP. Journal of Geophysical Research: Space Physics, 112(A11) (2007).

[71] Liu, J., Jia, X., Zhu, Y., Xu, J., Fu, J., Zhang, R., He, Y.: Comparing GNSS TEC data from the African continent with IRI-2016, IRI-Plas, and NeQuick predictions. Advances in Space Research, 69(7), 2852-2864 (2022).

[72] Lockwood, M., Owens, M. J., Barnard, L. A., Haines, C., Scott, C. J., McWilliams, K. A., Coxon, J. C.: Semi-annual, annual and Universal Time variations in the magnetosphere and in geomagnetic activity: 1. Geomagnetic data. Journal of Space Weather and Space Climate, 10, 23 (2020).

[73] Lomidze, L., Knudsen, D. J., Shepherd, M., Huba, J. D., Maute, A.: Equinoctial asymmetry in the upper ionosphere: Comparison of satellite observations and models. *Journal of Geophysical Research: Space Physics*, *128*, e2022JA031123 (2023). https://doi. org/10.1029/2022JA031123.

[74] Luan, X., Wang, W., Burns, A., Solomon, S. C., Lei, J.: Midlatitude nighttime enhancement in F region electron density from global COSMIC measurements under solar minimum winter condition. Journal of Geophysical Research: Space Physics, 113(A9) (2008).

[75] McGranaghan, R. M., Mannucci, A. J., Wilson, B., Mattmann, C. A., Chadwick, R.: New capabilities for prediction of high-latitude ionospheric scintillation: A novel approach with machine learning. Space Weather, 16(11), 1817-1846 (2018).

[76] Mehmood, M., Filjar, R., Saleem, S., Shah, M., Ahmed, A.: TEC derived from local GPS network in Pakistan and comparison with IRI-2016 and IRI-PLAS 2017. Acta Geophysica, 69, 381-389 (2021).

[77] Mengistu, E., Moldwin, M. B., Damtie, B., Nigussie, M.: The performance of IRI-2016 in the African sector of equatorial ionosphere for different geomagnetic conditions and time scales. Journal of Atmospheric and Solar-Terrestrial Physics, 186, 116-138 (2019).

[78] Mohamed, B. E., Tawfik, H. S., Abdelfatah, M. A., El-Fiky, G. S.: Improvement of international reference ionospheric model total electron content maps: a case study using artificial neural network in Egypt. *Journal of Applied Geodesy*, (0) (2023). https://doi.org/10.1515/jag-2023-0002

[79] Mohammadi, M., Al-Fuqaha, A.: Enabling cognitive smart cities using big data and machine learning: Approaches and challenges. IEEE Communications Magazine, 56(2), 94-101 (2018).

[80] Muella, M. T. D. A. H., De Paula, E. R., Kantor, I. J., Batista, I. S., Sobral, J. H. A., Abdu, M. A., Smorigo, P. F.: GPS L-band scintillations and ionospheric irregularity zonal drifts inferred at equatorial and low-latitude regions. Journal of Atmospheric and Solar-Terrestrial Physics, 70(10), 1261-1272 (2008).

[81] Mukherjee, S., Sarkar, S., Purohit, P. K., Gwal, A. K.: Seasonal variation of total electron content at crest of equatorial anomaly station during low solar activity conditions. Advances in space Research, 46(3), 291-295 (2010).

[82] Nava, B., Coisson, P., Radicella, S. M.: A new version of the NeQuick ionosphere electron density model. Journal of atmospheric and solar-terrestrial physics, 70(15), 1856-1862 (2008).

[83] Obafaye, A. A., Okoh, D. I., Adewale, A. O., Udochukwu, B. C., Rabiu, A. B.: Comparison of IRI-01cor, IRI-Plas 2017, Ne Quick-2 and NIGTEC models with GPS-TEC measurements over Nigeria. Sun and Geosphere, 14(2), 147-160 (2019).

[84] Ogwala, A., Onori, E. O., Kayode, Y. O., Adele, R. A., Somoye, E. O.: The Equatorial Ionospheric phenomena: A review of past studies, government interest and unsolved problems. Latin-American Journal of Physics Education, 16(2), 3 (2022).

[85] Ogwala, A., Somoye, E. O., Ogunmodimu, O., Adeniji-Adele, R. A., Onori, E. O., Oyedokun, O.: Diurnal, seasonal and solar cycle variation in total electron content and comparison with IRI-2016 model at Birnin Kebbi. Annales Geophysicae, 37(5), 775–789 (2019). doi:10.5194/angeo-37-775-2019.

[86] Ogwala, A., Somoye, E.O., Panda, S.K., Ogundinmu, O., Onori, E.O., Sharma, S.K., Okoh, D., Oyedokun, O.J.: Total electron content at equatorial and low-, middle-and high-latitudes in the African longitude sector and its comparison with IRI-2016 and IRI-Plas2017 models. Advances in space research 68, 2160-2176 (2021). https://doi.org/10.1016/j.asr.2020.07.013.

[87] Okoh, D., Onwuneme, S., Seemala, G., Shuanggen, J., Rabiu, B., Nava, B.,Uwamahoro, J.: Assessment of the NeQuick-2 and IRI-Plas 2017 models using global and long-term GNSS measurements. Journal of Atmospheric and Solar-Terrestrial Physics 170 , 1–10 (2018).

[88] Okoh, D., Seemala, G., Rabiu, B., Habarulema, J. B., Jin, S., Shiokawa, K., Shetti, D.: A neural network-based ionospheric model over Africa from Constellation Observing System for Meteorology, Ionosphere, and Climate and Ground Global Positioning System observations. Journal of Geophysical Research: Space Physics, 124(12), 10512-10532 (2019).

[89] Oloketuyi, J., Liu, Y., Zhao, M.: The periodic and temporal behaviors of solar X-ray flares in Solar Cycles 23 and 24. The Astrophysical Journal, 874(1), 20 (2019).

[90] Panda, S. K., Gedam, S. S., Jin, S.: Ionospheric TEC variations at low latitude Indian region. Satellite Positioning-Methods, Models and Applications. Tech-Publisher, Rijeka, Croatia, 149-174 (2015a).

[91] Panda, S. K., Gedam, S. S., Rajaram, G., Sripathi, S., Pant, T. K., Das, R. M.: A multi-technique study of the 29–31 October 2003 geomagnetic storm effect on low latitude ionosphere over Indian region with magnetometer, ionosonde, and GPS observations. Astrophysics and Space Science, 354, 267-274 (2014).

[92] Panda, S. K., Gedam, S. S., Rajaram, G.: Study of Ionospheric TEC from GPS observations and comparisons with IRI and SPIM model predictions in the low latitude anomaly Indian subcontinental region. Advances in Space Research, 55(8), 1948-1964 (2015b).

[93] Panda, S. K., Reddybattula, K. D., Haralambous, H., Sharma, S. K.: Assessment of ionospheric variability from IRI-2016, SPIM-2017, and IGS-GIM using Digisonde and GPS observations over Cyprus. Astrophysics and Space Science, 365, 1-23 (2020).

[94] Pezzopane, M., Pietrella, M., Pignatelli, A., Zolesi, B., Cander, L. R.: Assimilation of autoscaled data and regional and local ionospheric models as input sources for real-time 3-D International Reference Ionosphere modeling. Radio Science, 46(05), 1-16 (2011).

[95] Pezzopane, M., Pignalberi, A., Nava, B.: On the low-latitude NeQuick topside ionosphere mismodelling: the role of parameters H0, g, and r. *Advances in Space Research* (2023). https://doi.org/10.1016/j.asr.2023.04.014.

[96] Pignalberi, A., Pezzopane, M., Themens, D. R., Haralambous, H., Nava, B., Coïsson, P.: On the analytical description of the topside ionosphere by NeQuick: Modeling the scale height through COSMIC/FORMOSAT-3 selected data. IEEE Journal of Selected Topics in Applied Earth Observations and Remote Sensing, 13, 1867-1878 (2020).

[97] Pilipenko, V., Yagova, N., Romanova, N., Allen, J.: Statistical relationships between satellite anomalies at geostationary orbit and high-energy particles. Advances in Space Research, 37(6), 1192-1205 (2006).

[98] Rabiu, A.b., Adewale, A.O., Abdulrahim, R.B., Oyeyemi, E.O.: TEC derived from some GPS stations in Nigeria and comparison with the IRI and NeQuick models. Advances in Space Research 53,1290–1303 (2014).

[99] Radicella, S. M., Nava, B.: NeQuick model: Origin and evolution. In Proceedings of the 9th International Symposium on Antennas, Propagation and em Theory (pp. 422-425). IEEE (2010).

[100] Radicella, S. M.: The NeQuick model genesis, uses and evolution. Annals of geophysics, 52(3-4), 417-422 (2009).

[101] Rama Rao, P. V. S., Niranjan, K., Prasad, D. S. V. V. D., Gopi Krishna, S., Uma, G.: On the validity of the ionospheric pierce point (IPP) altitude of 350 km in the Indian equatorial and low-latitude sector. In Annales Geophysicae (Vol. 24, No. 8, pp. 2159-2168). Göttingen, Germany: Copernicus Publications (2006).

[102] Rao, S. S., Chakraborty, M., Pandey, R.: Ionospheric variations over Chinese EIA region using foF2 and comparison with IRI-2016 model. Advances in Space Research, 62(1), 84-93 (2018).

[103] Reddybattula, D., Kumar Panda, S.: Performance Analysis of Quiet and Disturbed Time Ionospheric TEC Responses from GPS-based Observations, IGS-GIM, IRI-2016 and SPIM/IRI-Plas 2017 Models over the Low Latitude Indian Region. Advances in Space Research (2019). doi:10.1016/j.asr.2019.03.034.

[104] Reinisch, B. W., Huang, X., Galkin, I. A., Paznukhov, V., Kozlov, A.: Recent advances in real-time analysis of ionograms and ionospheric drift measurements with digisondes. Journal of Atmospheric and Solar-Terrestrial Physics, 67(12), 1054-1062 (2005).

[105] Shahzad, R., Shah, M., Ahmed, A.: Comparison of VTEC from GPS and IRI-2007, IRI-2012 and IRI-2016 over Sukkur Pakistan. Astrophysics and Space Science, 366(4), 42 (2021).

[106] Sharma, G., Champati Ray, P. K., Kannaujiya, S.: Ionospheric total electron content for earthquake precursor detection. Remote sensing of northwest Himalayan ecosystems, 57-66 (2019).

[107] Shubin, V. N., Gulyaeva, T. L.: Global mapping of total electron content from GNSS observations for updating IRI-Plas model. Advances in Space Research, 69(1), 168-175 (2022).

[108] Sivavaraprasad, G., Deepika, V. S., SreenivasaRao, D., Kumar, M. R., Sridhar, M.: Performance evaluation of neural network TEC forecasting models over equatorial low-latitude Indian GNSS station. Geodesy and Geodynamics, 11(3), 192-201 (2020).

[109] Sreekumar, S., Sripathi, S.: The role of LSWS (satellite traces) and low latitude Esb layers in causing the variability of ESF irregularities over Indian sector. Advances in Space Research, 62(1), 94-110 (2018).

[110] Stolle, C., Manoj, C., Lühr, H., Maus, S., Alken, P.: Estimating the daytime equatorial ionization anomaly strength from electric field proxies. Journal of Geophysical Research: Space Physics, 113(A9) (2008).

[111] Sunda, S., Sridharan, R., Vyas, B. M., Khekale, P. V., Parikh, K. S., Ganeshan, A. S., Bagiya, M. S.: Satellite-based augmentation systems: A novel and cost-effective tool for ionospheric and space weather studies. Space Weather, 13(1), 6-15 (2015).

[112] Talari, P., Panda, S. K.: Occurrences of counter electrojets and possible ionospheric TEC variations round new Moon and full Moon days across the low latitude Indian region. Journal of Applied Geodesy, 13(3), 245-255 (2019).

[113] Tariku, Y. A.: Comparison of performance of the IRI 2016, IRI-Plas 2017, and NeQuick 2 models during different solar activity (2013–2018) years over South American sector. Radio Science, 55(8), 1-17 (2020a).

[114] Tariku, Y. A.: Pattern of the variation of the TEC extracted from the GPS, IRI 2016, IRI-Plas 2017 and NeQuick 2 over polar region, Antarctica. Life Sciences in Space Research, 25, 18–27 (2020b). doi:10.1016/j.lssr.2020.02.004.

[115] Tariku, Y. A.: Validation of the IRI 2016, IRI-Plas 2017 and NeQuick 2 models over the West Pacific regions using the SSN and F10.7 solar indices as proxy. Journal of Atmospheric and Solar-Terrestrial Physics (2019). doi:10.1016/ j.jastp.2019.06.002.

[116] Tariq, M. A., Shah, M., Ulukavak, M., Iqbal, T.: Comparison of TEC from GPS and IRI-2016 model over different regions of Pakistan during 2015–2017. Advances in Space Research, 64(3), 707-718 (2019).

[117] Wang, N., Yuan, Y., Li, Z., Li, Y., Huo, X., Li, M.: An examination of the Galileo NeQuick model: comparison with GPS and JASON TEC. GPS solutions, 21, 605-615 (2017).

[118] Yasyukevich, Y. V., Yasyukevich, A. S., Ratovsky, K. G., Klimenko, M. V., Klimenko, V. V., Chirik, N. V.: Winter anomaly in NmF2 and TEC: when and where it can occur. Journal of Space Weather and Space Climate, 8, A45(2018).

[119] Yasyukevich, Y. V., Zatolokin, D., Padokhin, A., Wang, N., Nava, B., Li, Z., Vesnin, A.: Klobuchar, NeQuickG, BDGIM, GLONASS, IRI-2016, IRI-2012, IRI-Plas, NeQuick2, and GEMTEC Ionospheric Models: A Comparison in Total Electron Content and Positioning Domains. Sensors, 23(10), 4773 (2023).

[120] Zhang, M. L., Wan, W., Liu, L., Ning, B.: Variability study of the crest-to-trough TEC ratio of the equatorial ionization anomaly around 120 E longitude. Advances in Space Research, 43(11), 1762-1769 (2009).